COVID-19 infection spread and human mobility

Shibamoto, Masahiko
Hayaki, Shoka
Ogisu, Yoshitaka

(Citation)
Journal of the Japanese and International Economies,64:101195

(Issue Date)
2022-06

(Resource Type)
journal article

(Version)
Version of Record

(URL)
https://hdl.handle.net/20.500.14094/90009173

Journal of The Japanese and International Economies 64 (2022) 101195

Contents lists available at ScienceDirect

Journal of The Japanese and International Economies

journal homepage: www.elsevier.com/locate/jjie

COVID-19 infection spread and human mobility☆

Masahiko Shibamoto [a,*], Shoka Hayaki [b], Yoshitaka Ogisu [c]

[a] Research Institute for Economics and Business Administration (RIEB) and Center for Computational Social Science (CCSS), Kobe University, 2-1, Rokkodai, Nada, Kobe, 657-8501, Japan
[b] Graduate School of Business Administration, Kobe University, 2-1, Rokkodai, Nada, Kobe, 657-8501, Japan
[c] Graduate School of Economics, Kobe University, 2-1, Rokkodai, Nada, Kobe, 657-8501, Japan

ARTICLE INFO

JEL classification:
C32
E31
E32
I10

Keywords:
COVID-19
New infection cases
Infection–mobility trade-off
Mobility demand
Stochastic trend and cycle
macroeconometrics

ABSTRACT

Given that real-world infection-spread scenarios pose many uncertainties, and predictions and simulations may differ from reality, this study explores factors essential for more realistically describing an infection situation. It furnishes three approaches to the argument that human mobility can create an acceleration of the spread of COVID-19 infection and its cyclicality under the simultaneous relationship. First, the study presents a dynamic model comprising the infection–mobility trade-off and mobility demand, where an increase in human mobility can cause infection explosion and where, conversely, an increase in new infections can be made temporary by suppressing mobility. Second, using time-series data for Japan, it presents empirical evidence for a stochastic trend and cycle in new infection cases. Third, it employs macroeconometrics to ascertain the feasibility of our model's predictions. Accordingly, from March 2020 to May 2021, the sources of COVID-19 infection spread in Japan varied significantly over time, and each change in the trend and cycle of new infection cases explained approximately half the respective variation.

1. Introduction

Many epidemiologists have sounded alerts regarding the COVID-19 infection spread, ever since the initial outbreak in early 2020. They have conducted detailed analyses of the pandemic situation from the primary stages. For instance, the results of the Susceptible-Infected-Recovered (SIR) model, a benchmark for modeling epidemics in the field, hinted at the likelihood of a pandemic. Moreover, in February and early March 2020, the models predicted exponential growth, massive infections, hospitalizations, and deaths.[1] The models further suggested that either eliminating physical contact between people, to reduce the probability of being infected, or inducing herd immunity, where infected persons come into contact with sufficient people who have recovered from or have become immune to the infection, can slow the infection spread at a fixed reproduction rate. Thus, relevant bodies opted for the former approach, by imposing restrictions on mobility and in-person economic activities to alleviate a possible COVID-19-related tragedy.[2]

Unsurprisingly, predictions regarding COVID-19 infection spread

☆ We extend our special thanks to Takashi Kamihigashi, Ryuzo Miyao, and Masato Shizume for their extensive help and encouragement in the writing of this paper. We are also grateful to Kenya Fujiwara, Nobuaki Hamaguchi, Ken-ichi Hashimoto, Tomoko Hashino, Takahiro Sato, the seminar participants at Kobe University, and two anonymous referees for helpful comments and discussions. This study received financial support from the Japan Society for the Promotion of Science (JSPS KAKENHI Grant Number 20H05633 and 21K01579) and JST-Mirai Program, Japan (Grant Number JPMJMI20B4).

* Corresponding author.
E-mail addresses: shibamoto@rieb.kobe-u.ac.jp, masa-shiba@hotmail.co.jp (M. Shibamoto), 179b011b@stu.kobe-u.ac.jp (S. Hayaki), 197e109e@stu.kobe-u.ac.jp (Y. Ogisu).

[1] In Japan, on February 24, 2020, members of the Expert Committee on Countermeasures to Combat Infectious Diseases of Novel Coronaviruses posited that the infection in Japan could spread rapidly. https://www.mhlw.go.jp/stf/seisakunitsuite/newpage_00006.html (Accessed June 12, 2021)

[2] As per the Expert Committee on Countermeasures against Novel Coronavirus Infections report on February 24, 2020, the committee sought a policy that reduces the speed of the rise in infection cases and lowers the peak of the epidemic wave, while strengthening the medical response system. https://www.kantei.go.jp/jp/singi/novel_coronavirus/senmonkakaigi/sidai_r020224.pdf (Accessed June 12, 2021)

https://doi.org/10.1016/j.jjie.2022.101195
Received 4 October 2021; Received in revised form 31 January 2022; Accepted 2 February 2022
Available online 12 February 2022

garnered much attention because anxieties and fears were strong amid extensive reporting of the outbreak by the media in early 2020. Epidemiological experts, researchers, and commentators have since disseminated knowledge and opinions in various media, closely following the evolution of the spread into the current long-running pandemic.[3]

However, epidemiological model predictions and simulations are not necessarily consistent with reality. For example, in Japan, the number of new infection cases did not increase as expected during the first wave of the pandemic. Even though infection cases may have decreased because of the mobility restrictions and the subsequent declaration of the first state of emergency by the government, the number of new infection cases did not decrease easily during the third and fourth waves, despite the further restrictions of the second and third state of emergency declarations. To be sure, real-world scenarios pose many uncertainties, and predictions and simulations may differ from reality if assumptions change. However, to inform relevant policies and contribute to the literature, it is worthwhile to explore factors essential for a more realistic description of the evolution of an infection situation.

Arguably, COVID-19 infection cases are closely linked to human mobility. Accordingly, the rise in new infection cases is *positively* associated with human mobility because the probability of being infected via interaction with other infected people increases as mobility increases. However, people *curb* their mobility in response to the infection situation. Thus, whenever the number of new infection cases increases, people will restrict their mobility. Therefore, a simultaneous relationship between human mobility and new infection cases likely underlies the dynamics of an infection spread.

Hence, this study explores the dynamics of the COVID-19 infection and human mobility, to explain the reality of the COVID-19 spread via the underlying simultaneous relationship. In particular, the supply side of the COVID-19 infection spread and demand side of human mobility, are likely to determine the number of new infection cases endogenously. Thus, human mobility can create a dire situation. That is, given a rising number of new infection cases, unregulated economic activities can induce an explosive increase in such cases. However, systemic mechanisms can converge the increase or decrease in the number of new infection cases. When people respond to the current infection situation and refrain from activities, the effective reproduction rate changes systematically according to their behavior and stabilizes, relative to the standard SIR model prediction.

Under the presence of the simultaneous relationship, an unexpected observed increase in new infection cases can produce different predictions for infection spread, depending on the underlying factors. As the infectivity of the virus changes over time with the emergence of variant strains, the infection risk changes as well; hence, the number of new infections can suddenly increase. If people are sufficiently aware of and sensitive to changes in infection risk and change their behavior to avoid infection, the infection spread can be expected to be transient. In contrast, if people's patience with the infection situation is limited and their behavioral preferences change so that they are less sensitive to changes in infection risk, the infection spread is expected to be prolonged. Therefore, the key challenge in predicting infection spread is to monitor not only changes in the infection risk itself, but also the changes in people's perception of the risk.

The 2020–2021 outbreak situation in Japan is a valuable example to explore the role of human mobility in COVID-19 infection cases empirically. Unlike China, the US, and European countries that imposed mandatory lockdowns, the Japanese government has not legally restricted social activities owing to the spread of COVID-19, but has simply asked people to refrain from going out and closed restaurants during the declared emergency.[4] Nevertheless, COVID-19-infection status in Japan has been and remains lower than in most other countries. As of May 21, 2021, the total number of confirmed cases in Japan was approximately 700,000, less than 1% of the total population. However, the spread of the infection has profoundly impacted the economy; Japan's real GDP in 2020 was down by 4.8% from the previous year, the second-largest drop on record, after the recession in 2009 due to the global financial crisis. This situation suggests that despite the absence of legal or behavioral restrictions, people in Japan tend to voluntarily restrict their behavior in response to infection spread, at the expense of economic gain.

This study contributes to the literature in three ways. First, it conducts a model analysis of the dynamics of new infection cases. In particular, it emphasizes the role of mobility demand. Changes in human behavior preferences, such as familiarity with and ignorance of the pandemic, can accelerate infection spread. However, a systematic response of mobility demand to sudden changes in new infection cases can induce cyclicality of such cases. Second, the study presents empirical evidence of a stochastic trend and cycle in new infection cases. Third, this study employs macroeconometrics to present findings supporting the argument in the model analysis. Further, sources of the COVID-19 infection spread vary significantly over time, and the changes in the trend and cycle of new infection cases explain approximately half the respective variation, from February 2020 to May 2021 in Japan.

The rest of this paper is organized as follows. Section 2 reviews the literature relevant to this study. Section 3 presents a model analysis of new COVID-19 infection dynamics. Section 4 introduces the time-series data and shows the time-series features on the number of new COVID-19 infection cases. Section 5 presents empirical results via macroeconometric analysis. Section 6 discusses the findings and concludes the study. The Appendix provides data sources and weekly data construction. The Online Appendix provides additional analyses, and reports the robustness check and sensitivity analysis of the empirical results in the benchmark model.

2. Related work

Model prediction for equilibrium reproduction number equal to one

Several studies (e.g., Gans, 2020) present theoretical models that can generate the tendency toward an equilibrium point, where the reproduction number is equal to one. Such works are inspired by the regularity in the reproduction number pattern, showing a sudden rise and subsequent fall to approximately one or just below one (not zero), that has been documented across all states in the US and many countries worldwide, documented by Atkeson et al. (2020). The key mechanism underlying the equilibrium reproduction number equal to one in the model, is that individuals can base their behavior on prevalence rather than the falling set of those who are susceptible, to slow an infection using the standard SIR model with a fixed reproduction rate. In this paper, we present a dynamic model by retaining its implication. We abbreviate the SIR part of the model for simplicity and specify the supply

[3] News items on COVID-19 on Nippon Hoso Kyokai (Japan Broadcasting Corporation), Japan's only public broadcaster, were 289 in January 2020, increased to 1,638 in February, and reached more than 4,000 in April. Monthly news stories have since been always approximately 2,000, as of June 2021.

[4] The stringency index, calculated by the Oxford Coronavirus Government Response Tracker project, is a measure of the strictness of government policies and provides evidence that policy impact in Japan is extremely low. On average, Japan's stringency index during the sampling period was 39.9, the seventeenth lowest among the 181 countries for which data can be obtained. Moreover, it is the second lowest among Organisation for Economic Co-operation and Development member countries after New Zealand (36.9) and the second lowest among countries with a population of 50 million or more after Tanzania (21.8). The global average of the stringency index is 59.1, and the population-weighted global average is 66.1. The index in major countries such as Brazil (68.6), Canada (68.6), China (71.9), France (65.0), Germany (66.4), India (74.6), Italy (71.8), Russia (53.9), the UK (70.2), and the US (66.1) is generally high.

side of new infection cases, to capture a trade-off between the new cases as something undesirable and human mobility. Further, we emphasize the role of mobility demand to generate the stochastic trend and cycle in the new infection cases.

Time-series analysis for the COVID-19 infections

Time-series modeling considers the model that captures the non-stationary nature of the infection spread in the dynamics of new infection cases. Jiang et al. (forthcoming) develop the self-normalization technique to capture the phase transitions of an epidemic growth rate via multiple change-points and apply it to the log of the cumulative COVID-19 confirmed cases and deaths. They argue that the forecasts using time-series modeling can be a meaningful addition to the other forecasting models, including complex mechanistic models for tracking the COVID-19 pandemic. While their model characterizes the non-stationary nature of the infection spread as the piecewise linear trend, we consider time-series modeling that does the same as a stochastic trend. Specifically, we provide empirical evidence of a stochastic trend and cycle in the log of the new infection cases and apply the vector autoregressive (VAR) model comprising the log changes in such cases and the measure of human mobility to investigate the role of the trend and cycle.[5]

Forecasting and simulating COVID-19 infections using complex mechanistic models

Many studies have generated COVID-19 infection forecasts and simulations. In particular, epidemiological models, such as the SIR model, are commonly used for estimations and predictions to quantify knowledge (or the absence of it) on the current infection status, and generate simulations to explore suggestions for policymakers (Kissler et al., 2020; Atkeson, 2020). Arik et al. (2020) propose complex mechanistic models modifying epidemiological models, such as the Susceptible-Exposed-Infectious-Removed model, by means of information-bearing covariates using machine learning and artificial intelligence. This study does not aim to explore or provide a better forecasting model than other proposed forecasting methods. Rather, it focuses on investigating the role of human mobility in COVID-19 dynamics, using a model that can capture the dynamics of the number of new infection cases and human mobility.

Epidemiological models with human behavior

Following the seminal work by Eichenbaum et al. (2021), many studies are increasingly incorporating epidemiological SIR models into economic analysis; these are often referred to as the SIR–Macro models. Regarding Japan, Kubota (2021) and Hosono (2021) present the models with different ingredients per their interests. They mainly focus on the effect of the spread of COVID-19 infection on economic activities, using the dynamic stochastic general equilibrium models. In contrast, this study primarily examines the role of human mobility in the dynamics of the new infection cases using macroeconometric models.

Empirical evidence on the association between the COVID-19 infection and human mobility

Many empirical studies have demonstrated a significant relationship between COVID-19 infection status and human mobility using various data sources. They conduct an empirical analysis for each of the two causal relationships between human mobility and the number of new infection cases. Some studies report empirical evidence supporting a trade-off between human mobility and COVID-19 infection. For example, Kraemer et al. (2020) use rich data on COVID-19 infection cases (including the dates when people first reported symptoms) and real-time travel data in China, and find that mobility measures offer a precise prediction of COVID-19 spread in Chinese cities at the start of 2020. In Japan, Nagata et al. (2021) estimate the impact of mobility changes on the new confirmed cases using mobile device data and argue that mobility changes, especially in areas active at night, were positively and significantly associated with COVID-19 spread. Moreover, Fujii and Nakata (2021) and Fukao and Shioji (2022) use daily data on the Google mobility index and the number of new infection cases to analyze the determinants of reproduction rate and mobility.[6] Others report the response of human mobility to new infection cases. For example, Goolsbee and Syverson (2021) use mobile phone data in the US between March and May 2020, to compare the reductions in visits to businesses between counties that were in government-mandated lockdown states with those in non-lockdown states. They find that the reductions in visits primarily stemmed from peoples' choices; those attributable to a government-mandated lockdown were few. Further, Watanabe and Yabu (2021) use a daily prefecture-level mobile device data to examine the degree of voluntary response to infection cases in Japan and find results quantitatively and qualitatively similar to Goolsbee and Syverson (2021).[7] This study conducts empirical analyses using the macroeconometric model comprising a system of simultaneous equations that considers the two causal relationships between human mobility and the number of new infection cases.[8]

3. Rationale for the existence of both a stochastic trend and cycle in the dynamics of the COVID-19 infection

This section explains the logic behind our argument that while an increase in human mobility can cause infection explosion, such an increase in new infections can be made temporary by suppressing mobility.[9] Specifically, we present the analysis using a straightforward model for the dynamics of new COVID-19 infection cases, comprising a system of simultaneous equations that considers the two causal relationships (i.e., the infection–mobility trade-off and mobility demand). Our model can produce a stochastic trend and cycle of new infection cases under certain conditions.

3.1. The dynamic model of the COVID-19 infection and human mobility

We consider a model that can describe COVID-19 infection dynamics and human mobility. The variable π_t represents the new infection cases

[5] The VAR model yields consistent estimates even if each variable in the model is non-stationary. See Hamilton (1994) pp.651-653.

[6] Fujii and Nakata (2021) connect SIR dynamics with economic activity, though they do not incorporate optimization of economic agents in their analysis, unlike the studies by (for example) Eichenbaum et al. (2021).

[7] Watanabe and Yabu (2021) refer to the voluntary lockdown as refraining from going out by choice, which is different from the mandatory lockdowns by governments in China, the US, and European countries.

[8] Although this study has different objectives relative to prior studies, the closest study to this work is the one by Fukao and Shioji (2022) in that they regress each of the system comprising the infection–mobility trade-off (i.e., the pandemic Phillips curve) and mobility demand (i.e., the pandemic IS curve and pandemic Taylor rule).

[9] The purpose of this section is not to propose a model which is suitable for real-world applications, such as predicting or simulating the infection spread.

at time t, defined as the log of new confirmed COVID-19 infection cases. The variable y_t represents the mobility level chosen by people at time t, defined as the log deviation from the steady state.[10]

First, we model the causal relationship representing an infection–mobility trade-off. Specifically, we consider the new infection production function as follows:

$$\pi_{t+1} = \pi_t + \kappa y_{t-1} + \epsilon_{\pi,t+1}, \tag{1}$$

where $\kappa > 0$ is the parameter, and $\epsilon_{\pi,t}$ is the stochastic term of the new infection production function. Eq. (1) can easily express an infection–mobility trade-off, where new infection cases, as something undesirable, are positively associated with human activities. Further, in the formulation of Eq. (1), a new infection case at time $t+1$, π_{t+1}, is regarded as a function of human mobility two terms prior, y_{t-1}. This development reflects "epidemiological rigidity," which is the time lag between physical contact with infected people and COVID-19 infection (including worsening symptoms after an incubation period, diagnosis, testing, and reporting). We assume the time lag to be two weeks in the modeling.[11]

Now consider that there are two types of shocks related to new infection case at time t, denoting $\epsilon_{p,t}$ and $\epsilon_{c,t}$ respectively. We then decompose the stochastic term of the new infection production function as $\epsilon_{\pi,t} = \epsilon_{p,t} + \epsilon_{c,t}$. Regarding each shock process, we assume that

$$\epsilon_{i,t} = \rho_i \epsilon_{i,t-1} + \xi_{i,t}, \quad \rho_i \in [0,1], i \in \{p,c\}, \tag{2}$$

where each $\xi_{i,t}$ is independently and identically distributed with mean-zero, and is independent of each other. We will consider that people's responses to new infection cases vary across shocks, as shown below.

Next, we model the systematic response of human mobility demand, as people decide their mobility level by observing the latest number of new infection cases. Given the premise of the availability of information on the new infection cases at time t, we specify the mobility demand function as follows:

$$y_t = b(\pi_t - \pi_t^*), \tag{3}$$

where $b < 0$ denotes the parameter representing the sensitivity of mobility demand to the infection situation. Eq. (3) expresses the demand of people's mobility where people negatively change their mobility demand in response to the outbreak situation. In particular, mobility demand systematically responds to the deviation in new infection cases from its reference level. π_t^* is the *reference level of crowds*. From (3), the reference level works as a threshold of the activity level to react; if the number of new infection cases increases (decreases) above (below) the reference level, people refrain from their activities (become active).

We relate the degree of people's patience about the COVID-19 situation to the dynamics of the reference level. In practice, as the constrained lifestyle owing to the COVID-19 pandemic is prolonged, infection anxiety weakens: this phenomenon is often called Corona habituation. As reports of high numbers of new infection cases lead people to assume an air of permanence, people begin to entertain the thought that they "deserve it," even as the infection situation worsens.[12] Thus, to incorporate the degree of people's patience toward the infection situation into the model, we parameterize the reference level in Eq. (3) of the mobility demand as follows:

$$\pi_t^* = d\bar{\pi}_t, \tag{4}$$

where $d > 0$ denotes the parameter representing the degree of people's patience and $\bar{\pi}_t$ is the potential and trend level of the number of new infection cases, which are time-varying given $\epsilon_{p,t}$, following $\bar{\pi}_t = \bar{\pi}_{t-1} + \epsilon_{p,t}$. In $d = 1$, the reference level of new infection cases is neutral to their potential and trend level. In $d > 1$, people are not patient toward infection cases. As the long-term level of new infection cases increases, the reference level rises above the potential level, as described by Corona habituation. In $d < 1$, people are conservative about infection cases. Even if the long-term level of new infection cases rises even higher, people do not change their reference level drastically.

In our model setting, the change in new infection cases given $\epsilon_{p,t}$ is associated with a shock in mobility demand. We incorporate the degree of people's patience about the infection situation into the mobility demand in the model

$$y_t = b\pi_t - bd\bar{\pi}_{t-1} - bd\epsilon_{p,t}, \tag{5}$$

by substituting Eq. (4) into Eq. (3). Regarding $d > 1$, the increase in new infection cases given $\epsilon_{p,t}$ results in an *increase* in mobility demand, separate from its systematic response. Despite the increasing number of new infection cases, people aggressively continue their economic activities. However, regarding $0 < d < 1$, the increase in new infection cases given $\epsilon_{p,t}$ results in a *decrease* in mobility demand. Although they increase their reference level, people partially refrain from activities as per the infection situation. Moreover, regarding $d = 1$, people's behavior remains unchanged despite the rise in new infection cases given $\epsilon_{p,t}$, since their reference level also rises by the same amount.

Here, we analytically investigate the dynamic properties of the system. Replacing y_{t-1} in Eq. (1) by Eq. (3) generates

$$\Delta\pi_{t+1} = \kappa b(\pi_{t-1} - \pi_{t-1}^*) + \sum_{i\in\{p,c\}} \epsilon_{i,t+1}. \tag{6}$$

Eq. (6) means that when the number of new infection cases two weeks ago is above (below) the reference value, the current number of new infection cases is decreasing (increasing).

The model suggests that the change in new infection cases due to the infection shock ϵ_c is temporary. Replacing π_{t-1}^* in (6) by $\pi_{t-1}^* = d\bar{\pi}_{t-1} = d\sum_{\tau=1}^{t-1}\epsilon_{p,\tau}$ under the assumption of the initial value of $\bar{\pi}_0 = 0$ generates

$$\Delta\pi_{t+1} = \kappa b\pi_{t-1} - \kappa bd\sum_{\tau=1}^{t-1}\epsilon_{p,\tau} + \sum_{i\in\{p,c\}}\epsilon_{i,t+1}. \tag{7}$$

This relationship can also be described as a downward-sloping line given that $\Delta\pi_{t+1}$ is a function of π_{t-1}, as in the left panel of Fig. 1. The steady state of the new infection cases is where $\Delta\pi_{t+1} = 0$, which occurs at $\pi^s = d\sum_{\tau=1}^{t-1}\epsilon_{p,\tau}$.[13] Since ϵ_c does not affect the steady state, the change in

[10] In the model economy, we assume weekly frequency for the duration of time t.

[11] Lauer et al. (2020) report that the median incubation period is 5.1 days and that 97.5% of people develop symptoms within 11.5 days. Thus, it takes approximately a week from the time of infection to the time one develops symptoms; further, it takes a certain number of days after the actual symptoms appear for those infected to go to the hospital and undergo tests, after which the test results are reported. In practice, as per the announcement by the Japanese government of the basic policy on countermeasures against COVID-19 infections, the average time between the date of the onset to the date of the patients' diagnosis (reported until the early stage of the COVID-19 pandemic at the end of March 2020) was 9.0 days, though this seemed rather short at the time of preparing this paper. https://www.kantei.go.jp/jp/singi/novel_coronavirus/th_siryou/kihon_h_0525.pdf (Accessed June 14, 2021)

[12] Kuga (2021) reports the results of an empirical analysis of the status of Corona habituation in Japan. Specifically, the researcher quantitatively analyzes the state of people's COVID-19 anxiety using the "Survey on Changes in Daily Life Due to the New Coronavirus" (『新型コロナウイルスによる暮らしの変化に関する調査』), conducted by the Nissay Research Institute every three months since June 2020 on approximately 2,000 men and women aged 20 to 69 nationwide. The author notes that, relative to September 2020, when the second wave had passed, infection fears had weakened in late March 2021, despite a significant increase in the size of the infected population.

[13] We can derive the steady state of human mobility $y^s = 0$.

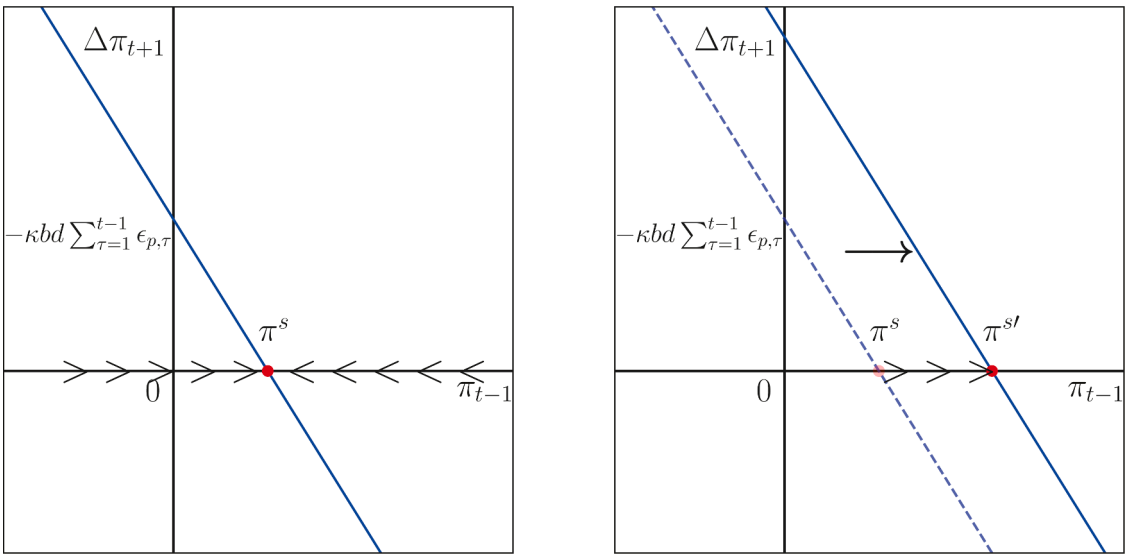

Fig. 1. Dynamics of the new COVID-19 infection cases in the model, the effect of ϵ_c and ϵ_p. *Notes*: This figure shows a phase diagram describing the dynamics of new COVID-19 infection cases in our model. The left panel displays the effect of an increase in new infection cases due to the shock ϵ_c. The right panel displays the effect of an increase in new infection cases due to the shock ϵ_p.

infection cases given ϵ_c can be shown as movements along the horizontal axis: leftwards when $\pi > \pi^s$ and rightwards when $\pi < \pi^s$. Hence, the fluctuation due to infection shocks ϵ_c creates cyclicality in new infection cases in the model economy.

However, this study's model suggests that the infection shock ϵ_p can permanently impact new infection cases. The right panel of Fig. 1 illustrates this impact diagrammatically. The change in infection cases given ϵ_p generates a rightward shift in the line, representing a change in the stochastic trend of the new infection cases. π stabilizes at the new steady state $\pi^{s'}$ in the diagram. Thus, the fluctuation given ϵ_p is the source of the non-stationary nature of new infection cases in the model economy.

The model can also be used to understand how the explosive spread of new infection cases occurs. For simplicity, we assume that new infection cases are in a steady state at time $t = 0$, without losing generality. Consider that an infection shock ξ_p hits the system at time 1. From Eq. (7) with Eq. (2); we can then easily compute $\Delta\pi_1 = \xi_{p,1}$ and $\Delta\pi_2 = \rho_p\xi_{p,1} < \Delta\pi_1$. Meanwhile, the rise in new cases at time 3 is given by $\Delta\pi_3 = \{\rho_p^2 + \kappa b(1-d)\}\xi_{p,1}$. The rise in new infection cases can then re-accelerate (i.e., $\Delta\pi_3 > \Delta\pi_2$) if the parameter values in the system are satisfied with the following condition;

$$-b(d-1) > \frac{\rho_p(1-\rho_p)}{\kappa}. \tag{8}$$

Intuitively, Eq. (8) means that the new infection cases could form a hump-shaped curve with some delay if people's reaction to such cases is too sensitive ($|b|$ is sufficiently large) or people have a fairly impatient preference for new infection cases ($d > 1$ is large enough).

3.2. Numerical example

We illustrate the dynamic relationship between the new infection cases and human mobility using the dynamic model with given parameter sets. The system in our dynamic model can be summarized by the VAR form with vector $S_t = (\pi_t,\ \bar{\pi}_t,\ y_{t-1},\ \epsilon_{p,t},\ \epsilon_{c,t})'$, as follows:

Table 1
Parameters for the numerical example

κ	b	d	ρ_p	ρ_c
4	− 0.05	5	0.3	0.3

Notes: The entries show the values of the parameters in the dynamic model, summarized by the vector autoregressive form (9) in calculating the calibrated impulse responses of the variables in the model to infection shocks, ξ_p, ξ_c.

$$S_{t+1} = \begin{pmatrix} 1 & 0 & \kappa & \rho_p & \rho_c \\ 0 & 1 & 0 & \rho_p & 0 \\ b & -bd & 0 & 0 & 0 \\ 0 & 0 & 0 & \rho_p & 0 \\ 0 & 0 & 0 & 0 & \rho_c \end{pmatrix} S_t + \begin{pmatrix} 1 & 1 \\ 1 & 0 \\ 0 & 0 \\ 1 & 0 \\ 0 & 1 \end{pmatrix} \begin{pmatrix} \xi_{p,t+1} \\ \xi_{c,t+1} \end{pmatrix}. \tag{9}$$

We can then calculate impulse responses of the variables in the system under a given set of parameters to examine the dynamic causal effect of the infection shocks, $\xi_{p,t}$ and $\xi_{c,t}$.

Table 1 presents the selected parameters. As a benchmark, we set the parameter value of $\kappa = 4$, selected as per the empirical findings of Nagata et al. (2021). Moreover, we also set the parameter value of $b = -0.05$, selected based on the empirical findings of Watanabe and Yabu (2021). We set the value of d to be equal to 5 as a calibration benchmark by assuming a Corona habituation where people are impatient about the outbreak situation. We set the values of the autoregressive parameters, ρ_p and ρ_c, to be equal to 0.3, reflecting the persistence of infection shocks.

The upper and lower four panels of Fig. 2 show the calibrated dynamic effects of the two infection shocks, ξ_p, and ξ_c, respectively, on the variables in the model economy. The solid line with circles in each panel represents the calibrated impulse responses of up to 20 times to one unit of each infection shock at time 0.

The dynamic model with given parameter sets predicts that the infection shock ξ_p can induce the explosion of new infection cases, accompanied by increases in human mobility. From the upper-left panel of Fig. 2, new infection cases π increase exponentially, as suggested by

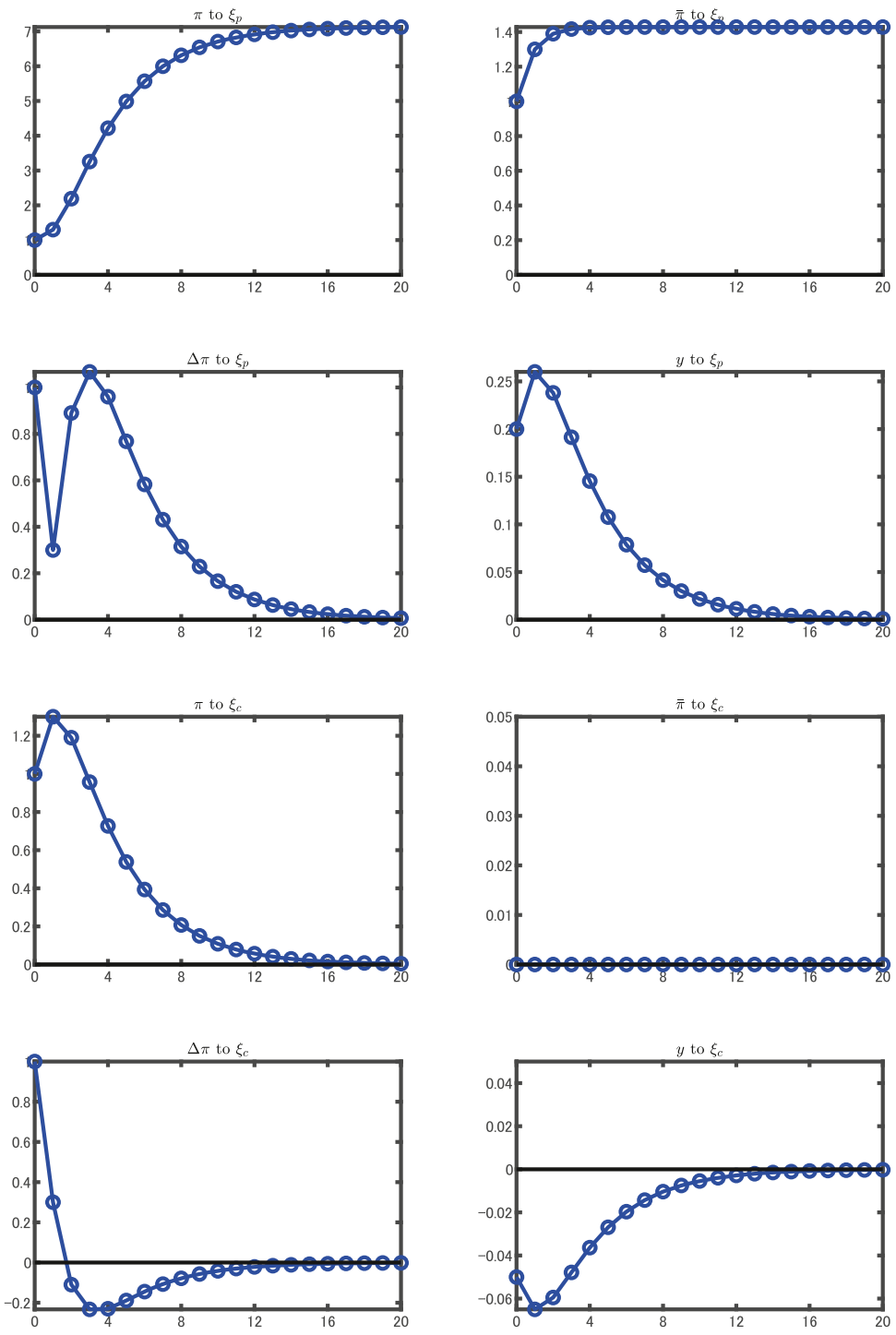

Fig. 2. Calibrated responses of variables in the model economy to the infection shocks, ξ_p and ξ_c. *Notes*: The solid line with circles in each of the upper and lower four panels represents the calibrated impulse responses to one unit of infection shocks, ξ_p and ξ_c, respectively. π: the log of new infection cases, $\bar{\pi}$: the potential and trend level of new infection cases, $\Delta\pi$: the log change in new infection cases, y: the mobility level, ξ_p, ξ_c: the infection shocks described in the text.

the SIR model. Further, the log change in the number of new infection cases $\Delta\pi$ shows a hump-shaped response with a second peak after some time, while leading to a sustained increase in human mobility y. Hence, in our model economy, the variation induced by the infection shock ξ_p results in an explosion of new infection cases that produces a stochastic trend, accompanied by a positive correlation between the new infection cases and human mobility.

In our model, an increase in human mobility, as per people's response to an outbreak situation, induces an infection explosion. Fig. 3 shows the comparison of the dynamic responses to the shock ξ_p with different values of parameter d representing the degree of people's patience about the infection situation. The dashed (dotted) line in each panel represents the responses with d as equal to one (d equal to 0.5). From the figure, the absence of mobility responses regarding $d = 1$ results in a limited rise in new infection cases relative to the benchmark, because the increase in reference levels π^* is comparable to the increase in the number of new infection cases $\pi, \bar{\pi}$ due to an infection shock ξ_p. Further, people's behavior remains unchanged. Additionally, regarding

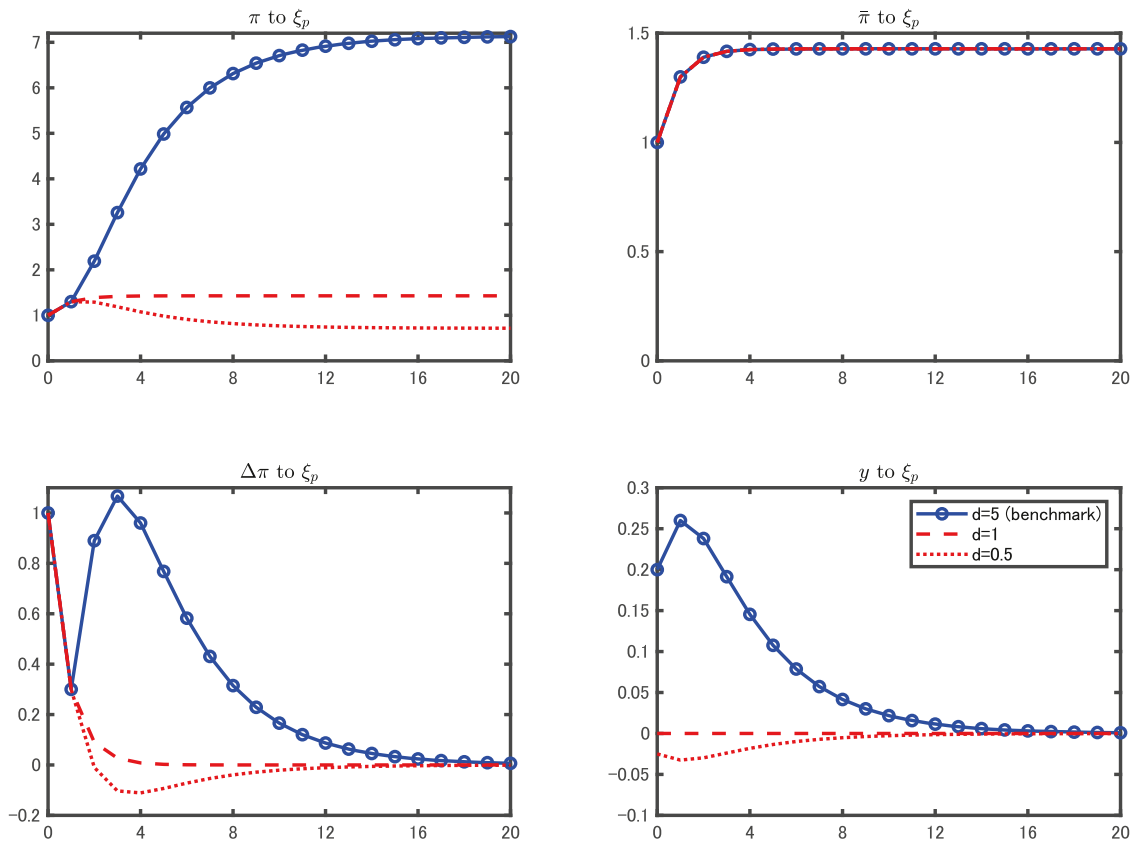

Fig. 3. Calibrated responses of variables in the model economy to the infection shock ξ_p with different sensitivities of reference levels. *Notes*: The solid line with circles, dashed line, and dotted line in each panel represent the calibrated impulse responses to one unit of infection shock ξ_p with different parameter values d, 5, 1 and 0.5, respectively. π: the log of new infection cases, $\bar{\pi}$: the potential and trend level of new infection cases, $\Delta\pi$: the log change in new infection cases, y: the mobility level, ξ_p: the infection shocks described in the text.

$d = 0.5$, as human mobility decreases, π converges to a level lower than 1, which is the impact immediately after the shock. Therefore, the model predicts that new infection cases can exponentially increase with a stochastic trend, due to increased human mobility associated with patience about the infection situation.

However, the increases in new infection cases induced by the shock ξ_c are temporary. From the lower four panels of Fig. 2, the new infection cases π eventually converge to zero after its transitory rise, while leading to a persistent decrease in human mobility y. Therefore, the fluctuation due to infection shocks ξ_c creates cyclicality in the new infection cases in the model economy.

The key mechanism underlying the cyclicality in new infection cases in our model is the mobility demand based on which people react to the increase in new cases by suppressing mobility. Fig. 4 shows the comparison of the dynamic responses to the shock ξ_c with different values of parameter b representing the systematic response of a mobility demand to the new infection cases. The red-dashed line in each panel represents the responses with b equal to zero. From the figure, the absence of mobility responses regarding $b = 0$ does not result in a steady decline in $\Delta\pi$ for the convergence of π to zero. Thus, a systematic response of mobility demand to changes in new infection cases is critical in the cyclicality of such cases in our model economy.

From our model, we can propose the following hypotheses to be examined empirically. The first is that there are, in reality, both a stochastic trend and cycle in new infection cases. The second is that there is a mixture of infection shocks that cause an infection explosion with increased mobility, and infection shocks that cause a temporary increase in new infection cases with decreased mobility. The third is that we can explain these differences in the impact of infection shocks in relation to the role of mobility demand; systematic changes of mobility demand in response to the infection spread, result in only a temporary increase in new infection cases, while exogenous changes in mobility demand have a persistent impact on new infection cases.

4. Evidence on the stochastic trend and cycle in new positive cases of the COVID-19 infection

This section presents evidence on the stochastic trend and cycle in new infection cases. We document the statistical time-series features of new positive COVID-19 infection cases in Japan. We especially focus on non-stationarity and cyclicality in infection spread.

We note the time-series data on COVID-19 spread in Japan during the sample period. Based on data availability, the sampling period is set from the week of February 16, 2020, to the week of May 9, 2021. The frequency of all data is weekly, and the sampling period spans up to 65 weeks. We constructed the weekly time series of confirmed new infection cases as the total cases over the week from Sunday to Saturday.[14]

First, we statistically examine the time-series characteristics of new infection cases. Table 2 shows the mean and standard deviation of the log changes in such cases. It reports the sum of the univariate autoregressive (AR) model coefficients with three-week lags for the log changes in new infection cases, as a measure of their persistence. Table 3

[14] The analysis focuses on the weekly time-series variation, as it does not include differences by day of the week, as in a daily series of the number of new infection cases.

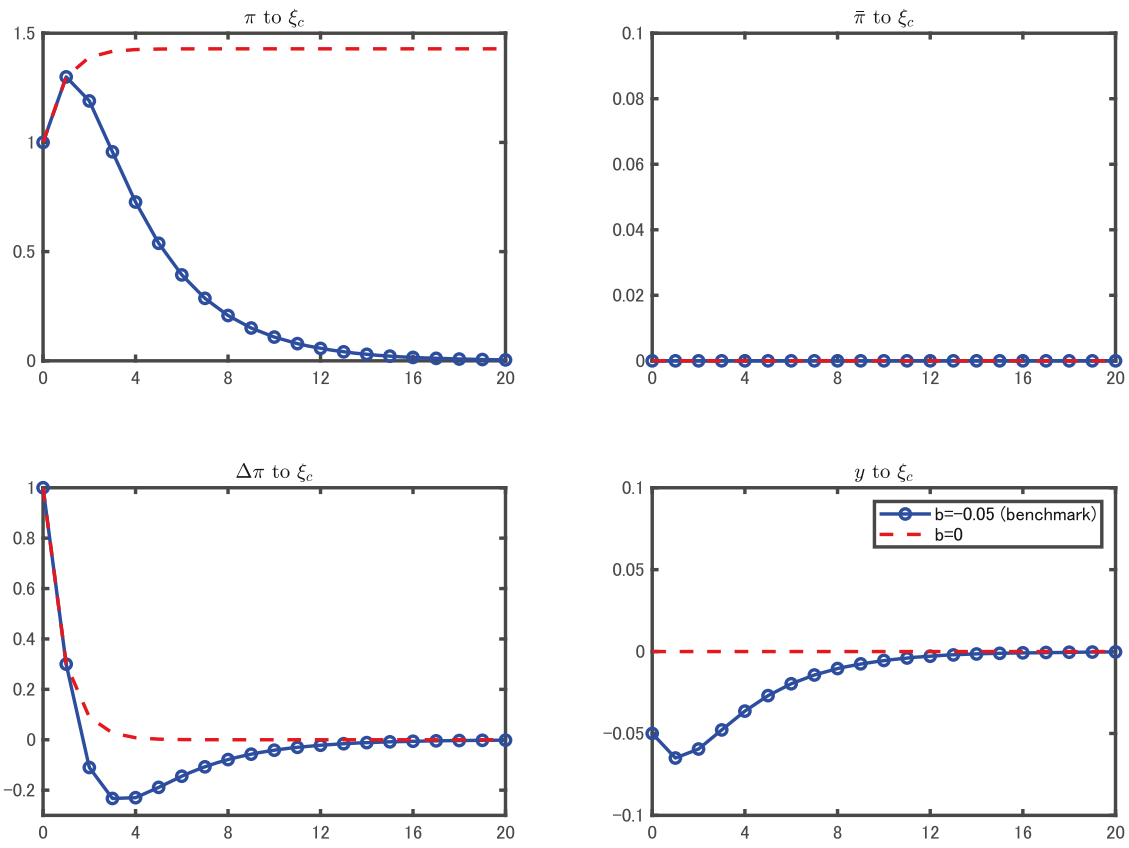

Fig. 4. Calibrated responses of variables in the model economy to the infection shock ξ_c with or without systematic responses of mobility demand. *Notes*: The solid line with circles and dashed line in each panel represent the calibrated impulse responses to one unit of infection shock ξ_c with the different parameter values b, -0.05, and 0, respectively. π: the log of new infection cases, $\bar{\pi}$: the potential and trend level of new infection cases, $\Delta\pi$: the log change in new infection cases, y: the mobility level, ξ_c: the infection shocks described in the text.

Table 2
Summary statistics for log change in new cases

	mean	std. dev.	persistence
Log change in new cases	0.098	0.364	0.585

Notes: This table shows the mean, standard deviation, and persistence measure of log change in new cases from the week of February 16, 2020, to the week of May 9, 2021. It reports the sum of the coefficients of the univariate autoregressive model with three-week lags for the log changes in the new infection cases as the persistence measure.

Table 3
Standardized long-run variance of log change in new cases

	Lag (k)					
	1	4	8	12	16	20
Standardized long-run variance	1.622	2.667	1.978	0.820	0.344	0.412
	(0.331)	(0.861)	(0.857)	(0.427)	(0.205)	(0.273)

Notes: This table shows the standardized long-run variance of log change in new cases from the week of February 16, 2020, to the week of May 9, 2021. The standardized long-run variance with k lag(s) is calculated as $1/(k+1)$ times the variance of $k+1$-differences of the log of the new infection cases, divided by the variance of its first difference. The numbers in parentheses are the Bartlett standard errors, calculated as $(4(k+1)/3T)^{.5}$ times standardized long-run variance.

shows the *standardized long-run variance* of the log *changes* as a measure of persistent fluctuations in the log *level* of new infection cases and its standard error, as proposed by Cochrane (1988).[15]

The summary statistics document the non-stationary nature of the log scale of the number of new infection cases. From Table 2, a historical average weekly rate of new infection cases is about 10%, but its deviation from the average is quite large over the sample period. More importantly, Table 2 shows that the persistence of log changes in new cases is 0.585; thus, the sudden increase in the new infection cases tends to persistently raise the reproduction rate. Hence, the number of infection cases in Japan can increase exponentially, as suggested by the SIR model.

However, the persistence measure for the log level of new cases suggests cyclicality as well as non-stationarity in new infection cases. Table 3 shows the standardized long-run variances of log change in new cases from lag 1 to lag 20; the values in parentheses are asymptotic standard errors. The standardized long-run variance is above one for a shorter horizon; for example, standardized long-run variance with lag $k = 1$ is above one and is statistically significant. Nonetheless, it is significantly below one for far longer horizons, such as lag $k = 20$. Thus, the fluctuation in the log level of new cases should have a cyclical

[15] See Cochrane (1988) for more details. The researcher proposes the ratio of far-future long-run variance of the *first difference* of the time-series variable of interest to its variance (we call the ratio the *standardized long-run variance*) as a measure of the persistence of the series *level*. This measure is zero for a stationary time series, one for a pure random walk, a number greater than one for a series that continues to diverge following a shock, and a number between zero and one for a series that returns to a stochastic trend in the future. The author estimates the long-run variance by $1/l$ times the variance of l-differences of the series.

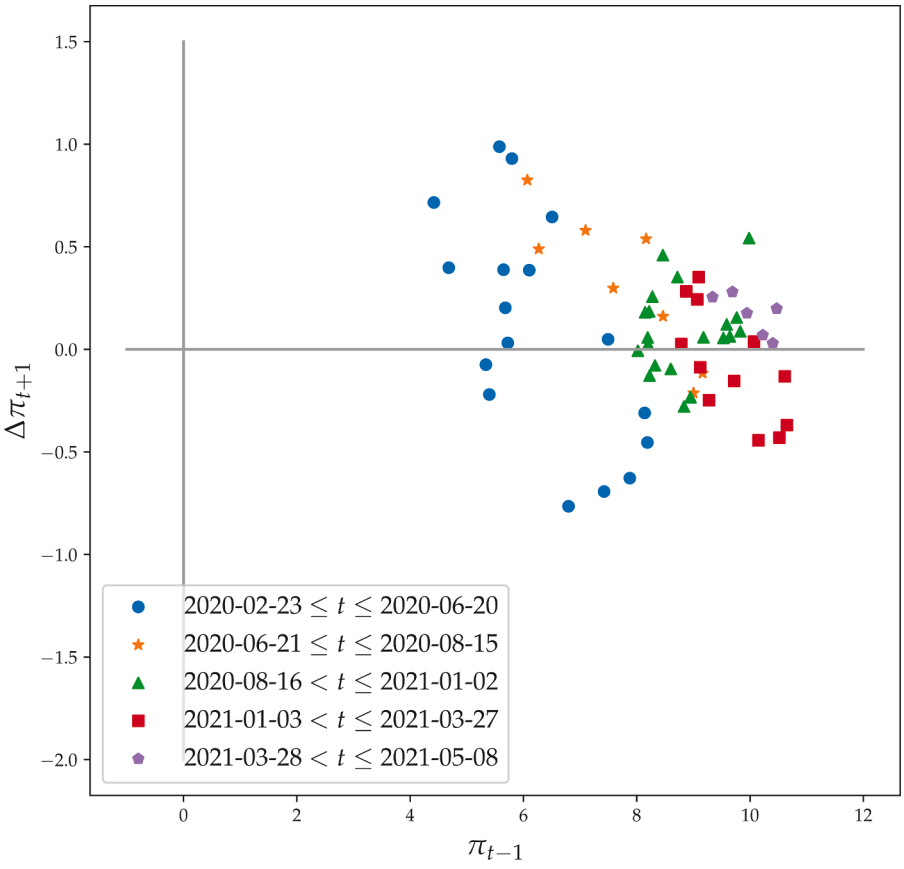

Fig. 5. Scatter plot of the log changes and levels in infection cases. *Notes*: The sample period spans from the week of February 23, 2020, to the week of May 2, 2021. Blue circles indicate the scatter plot of the one-week-ahead log changes in the number of COVID-19 infection cases and the one-week lag of its log levels, from the week of February 23, 2020 to the week of June 14, 2020. Orange stars indicate the plot from the week of June 21, 2020 to the week of August 9, 2020. Green triangles indicate the plot from the week of August 16, 2020 to the week of December 27, 2020. Red squares indicate the plot from the week of January 3, 2021 to the week of March 21, 2021. Purple pentagons indicate the plot from the week of March 28, 2021 to the week of May 2, 2021.

component, and the deviation following the component should return to a stochastic trend in the future.[16]

Next, we graph the dynamic properties of the log of COVID-19 new infection cases in reality. Fig. 5 shows the scatter plot of the one-week-ahead log changes in the number of COVID-19 infection cases and the one-week lag of its log levels, which is a sample analogous to Fig. 1.[17]

Although there does not seem to be much of a relationship between log changes and levels in the new infection cases over the entire sample period, we can identify some informative patterns by separating the periods. In particular, the scatter plot appears to depict a downward-sloping line for each subsample, which implies a cyclicality in the new infection cases in our dynamic model in Section 3. This suggests that the number of new infections sometimes tended to return to a certain level. On the other hand, looking across the subsamples, the downward-sloping line appears to have shifted to the right, especially around mid-2020, which implies a change in the stochastic trend of the new infection cases in the dynamic model. This suggests that the infection spread was long-lasting, depending on the time of year.

5. Macroeconometric analysis

In this section, we employ macroeconometrics to examine whether the data support the prediction in our model analysis of Section 3. Specifically, we use the VAR model to specify the joint dynamics of COVID-19 infection cases and human mobility in reality.[18] Thus, this sectionpresents empirical evidence on the (1) the information content of human mobility for the COVID-19 infection dynamics, (2) dynamic effect of the changes in the stochastic trend and cycle of the new infection cases, (3) role of human mobility in the dynamics of the new infection cases, (4) simultaneous equations system comprising the infection–mobility trade-off and mobility demand, and (5) application to the infection situation in Japanese prefectures.

5.1. *Information content of human mobility for the dynamics of the COVID-19 infection*

First, we examine the information content of human mobility for the COVID-19 infection dynamics. We measure the movement of people using six Google mobility indices (retail & recreation, grocery & pharmacy, parks, transit stations, workplaces, and residential), and then construct the composite index of mobility as the first principal component (PC) using six standardized (mean-zero and unit variance) mobility

[16] The standardized long-run variance reaches its peak with lag $k = 5$ and decreases from there. Since the standardized long-run variance reflects the cumulative autocorrelation, the autocorrelation begins a course toward negativity from around lag $k = 5$. This observation corresponds to the period from the peak-to-bottom of the number of new infection cases.

[17] We thank an anonymous referee for suggesting the following analysis.

[18] A possible alternative approach is to estimate the state space model derived from the dynamic model in Section 3. However, the model is very simple, so we have concerns about whether the model is valid with the actual data. The plausibility of the dynamic model with respect to actual data is a subject for future research.

Table 4
Information criteria for constant vs AR vs VAR models and F statistics for human mobility in equationfor new infection cases

Information criteria for the model:						$H_0 : y$ Fails	
VAR (3)		Hist. ave.		AR (3)		to Cause $\Delta\pi$	
AIC	BIC	AIC	BIC	AIC	BIC	Granger-*F*	
-2.68	-2.44	-2.02	-1.98	-2.36	-2.22	4.31	[0.04]

Notes: Information criteria indicate the log of the mean square forecast error for one-step model forecasts plus the penalty term for model complexity.AIC and BIC indicate the Akaike information criterion and Bayesian information criterion, respectively. For AIC, the penalty is $2/T$ times the number of parameters in the model equation. For BIC, the penalty is $\log(T)/T$ times the number of parameters in the model equation. Granger-F indicates the White (1980) heteroskedasticity-robust *F*-statistic for the Granger causality test under the null hypothesis that the coefficients on the one- to three-week lags of the composite index of mobility from the regression of log-changes in new infection cases in the reduced-form VARs are all equal to zero. The numbers in brackets are p-values for the Granger causality test. We set the lag length to three weeks in the AR and VAR estimation. Estimation samples span from the week of March 1, 2020, to the week of May 9, 2021.

indices, of which the unit is normalized to the unit of retail & recreation mobility index.[19] Although using more data and complicated models could generate a more accurate forecast of new infection cases, we expect the composite index of mobility as a representative measure for human mobility to contain significant information for the COVID-19 infection dynamics.

We consider the time-series model to capture the dynamics of new positive infection cases and human mobility. Specifically, we construct the following bivariate reduced-form VAR model:

$$X_t = a_0 + A_1 X_{t-1} + \cdots + A_p X_{t-p} + e_t, \tag{10}$$

expressed as

$$A(L)X_t = a_0 + e_t, \tag{11}$$

where $X_t = (\Delta\pi_t, y_t)'$ is a two-by-one vector comprising time-series variables of the log change in new positive cases $\Delta\pi_t$ and mobility measure y_t at week t, a_0 is a two-by-one constant vector, $A(L) = I - A_1 L - \cdots - A_p L^p$ is a pth order lag polynomial of a two-by-two coefficient matrix $A_j (j = 1, \cdots, p)$ and e_t is a two-by-one vector of serially uncorrelated innovation with a mean of zero and a covariance matrix of Σ_e.

The reduced-form weekly VAR model is estimated from the week of March 1, 2020, to the week of May 9, 2021. The lag length p in the reduced-form VAR estimation is set to three weeks. We confirm that taking three-week lags is sufficient to capture the system dynamics.[20]

We statistically confirm that human mobility plays an important role in constructing a time-series model of the dynamics of the number of new infection cases. Table 4 shows the results calculating Akaike and Bayesian information criteria (AIC and BIC, respectively) for the VAR and other candidate models. As other candidate models, we consider a historical average and a univariate AR with three-week lags.

From the perspective of model selection, there is statistical support for adding information on human mobility to the time-series model. We find that the VAR model has the smallest information criterion computed, whether AIC or BIC, of candidate models, which indicates the best model fit, including a penalty for complexity. This result suggests that the proposed VAR model with the lags of the composite index of mobility simply and thriftily captures the dynamics of the log changes in new infection cases.

Empirical evidence points to the significant information content of human mobility for new infection dynamics. The last column in Table 4 provides the *F* statistics for the Granger causality test under the null hypothesis that the coefficients on the one- to three-week lags of the composite index of mobility from the regression of log-changes in infection cases in the reduced-form VARs are all equal to zero. The *F* statistics show that the composite index of mobility contains valuable information for one-step model forecasts for new infection cases, which is statistically significant at the 5% level.[21]

5.2. Dynamic effect of the changes in stochastic trend and cycle of COVID-19 infection

In this subsection, we examine the role of "structural" shocks on COVID-19 infection cases and human mobility. In particular, we interpret fluctuations in COVID-19 infection cases and human mobility, as being attributable to changes in the stochastic trend and cycle underlying the time-series pattern of the infection cases. Accordingly, we consider two types of structural shocks: a shock with a permanent effect on the log level of new infection cases and a shock that causes temporary changes in new infection cases.[22] We identify two types of infection shocks, which are in reality mixed together. Thus, we examine whether it is consistent with the model prediction in section 3 that the former shock type increases mobility and the latter decreases it.

Let $\xi_{p,t}$ and $\xi_{c,t}$ be a permanent and non-permanent shock, respectively. In a structural VAR, the innovations e_t in (11) are assumed to be linear combinations of the structural shocks:

$$e_t = \Theta\xi_t, \tag{12}$$

where $\xi_t = (\xi_{p,t}, \xi_{c,t})'$, the elements of which are assumed to be independent of each other and have a unit variance, and $\Theta = (\Theta_p, \Theta_c)$ represents the impact matrix for the responses of the VAR variables X_t to the structural shocks ξ_t. Eqs. (11) and (12) yield a moving average representation regarding the structural shocks as follows:

$$X_t = b_0 + B(L)\Theta\xi_t, \tag{13}$$

[19] The weekly mobility index we use matches the median of each week of the daily mobility index, to eliminate the effects of holidays as much as possible. See the online appendixfor more details on the Google mobility indices and the data construction for the composite index of mobility.

[20] The Bayesian information criterion selects one lag, and the Akaike information criterion selects two lags. We perform a modified likelihood ratio test, proposed by Sims (1980), to check whether taking one or two lags is sufficient. The chi-squared statistics indicate that the null hypothesis of one or two lags is rejected at the 5% significance level against the alternative of three lags. They also indicate that conventional significance levels do not reject the null of three lags, as against the alternative of four lags. Moreover, the estimated results are insensitive when four and five lags are used.

[21] We confirm that the predictions of the VAR model improve over the AR model and the historical average for multistep-ahead model forecasts. In particular, although it has good predictive power in the shorter horizon, the predictive power of the AR model in the longer horizon is relatively poor. See the online appendixin more details for the comparison of in-sample forecasting accuracy among a historical average, AR model, and VAR model for the log-changes in new infection cases.

[22] We label a shock to the trend component of the new infection cases as a permanent shock and a shock to their cyclical component as a non-permanent shock. In our bivariate VAR model, the innovations in the reduced-form VARs are, by construction, decomposed into two structural shocks independent of each other. However, in reality, there can be other shocks than the ones we are interested in, such as idiosyncratic shocks that affect human mobility, unrelated to the number of new infection cases. In particular, the non-permanent shocks would be contaminated by such shocks, under the assumption that only a permanent shock affects the log level of new cases in the long run. They cannot be identified in our bivariate VAR model. We address this issue by using the composite index of mobility as a representative measure of mobility, so that the VAR model excludes as many idiosyncratic factors of mobility as possible. Nevertheless, it should be noted that our VAR model has such a limitation.

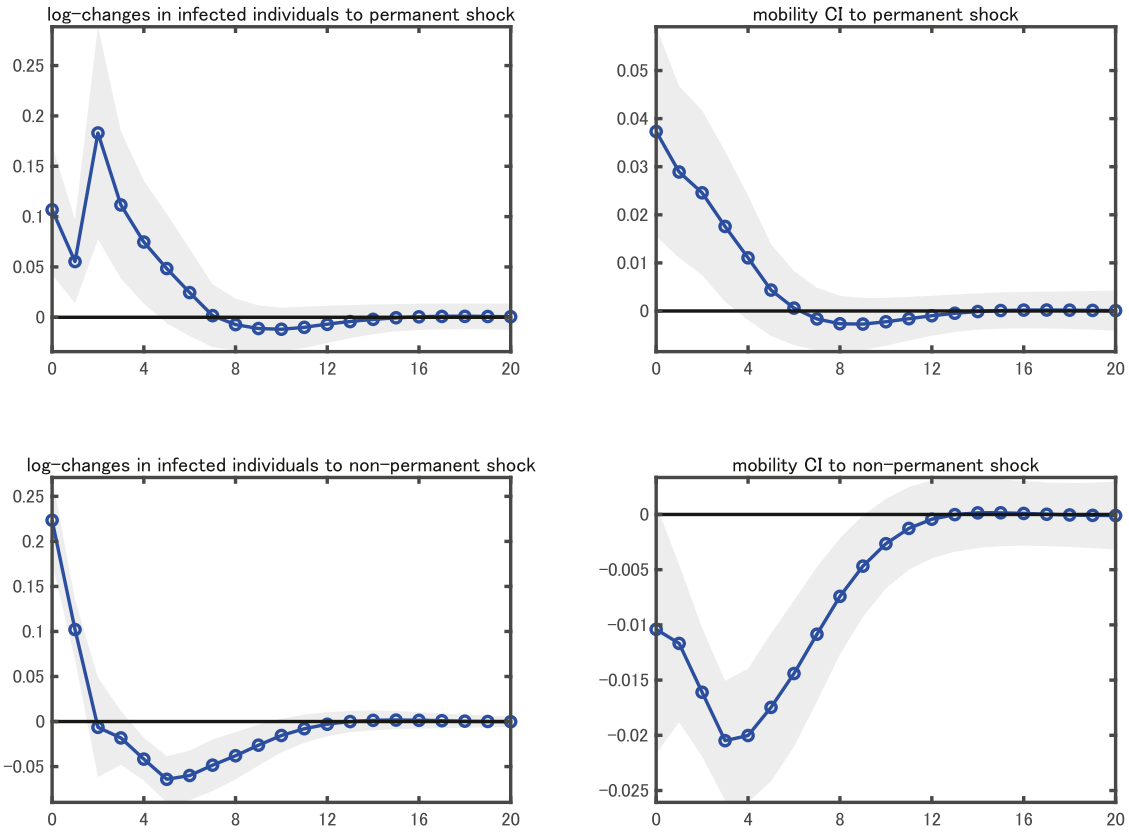

Fig. 6. Estimated responses of the log changes in infection cases and human mobility to permanent and non-permanent shocks. *Notes*: The solid line with circles in the upper and lower panels represent the point estimates of the impulse responses to one standard deviation permanent and non-permanent shock, respectively. The shaded areas denote one-standard-error bands, calculated using 1,000 bootstrap samples. Mobility CI denotes the composite index of mobility. We set the lag length to three weeks in the reduced-form vector autoregressive estimation. Estimation samples span from the week of March 1, 2020, to the week of May 9, 2021.

where $b_0 = A(L)^{-1}a_0$ and $B(L) = A(L)^{-1}$.

To identify Θ, we impose the long-run restriction on the VAR developed by Blanchard and Quah (1989) and King et al. (1991).[23] In particular, we assume that the non-permanent shocks do not affect the log level of new positive infection cases in the long run. This long-run restriction implies that the cumulative response of the log changes in new positive cases to the non-permanent shock, is constrained to zero:

$$[B(1)\Theta]_{12} = 0, \tag{14}$$

where $[B(1)\Theta]_{12}$ is the first row and second column of the matrix $B(1)\Theta$. The use of the restriction (14) with the long-run covariance matrix $B(1)\Sigma_e B(1)'$ identifies Θ. To determine the sign of the structural shocks, we assume that positive structural shocks have a positive impact on the log changes in infection cases, $\Theta_{1,p}, \Theta_{1,c} > 0$.

The estimated impulse response functions, $\widehat{B}(L)\widehat{\Theta}$, are summarized in Fig. 6. As described above, structural shocks are normalized to have unit variance and signed to positively affect the log changes in infection cases on impact. The solid line with the circles indicates the estimated response for the log changes and the composite index of mobility for up to 20 weeks. The shaded areas denote one-standard-error bands, calculated using 1,000 bootstrap samples.

Overall, this figure shows that structural shocks have a plausible effect, consistent with the dynamic model analysis discussed in Section 3. We find that the log changes in infection cases have a hump-shaped response to a permanent shock, with the second peak effect emerging after two weeks. Quantitatively, permanent shocks increase the *level* of new infections over the following eight weeks, by more than five times the impact, immediately after the shock. Moreover, human mobility rises in response to a permanent shock. However, a non-permanent shock, which raises the log changes in infection cases for two weeks and declines steadily for about eight weeks, induces a persistent decrease in human mobility to its lowest values, approximately four weeks after the shock occurs.

Next, we report the time series of structural shocks identified using the VAR model. In particular, it is useful to decompose the unexpected changes in COVID-19 infection cases into changes in the stochastic trend and in the cycle. Based on our model in section 3, we expect that permanent shocks would capture exogenous changes in people's demand for human mobility that deviates from systematic responses to infection risk, such as changes in behavioral preferences like Corona habituation and emergency restrictions on mobility due to certain prevalence measures by the government. On the other hand, we expect that non-permanent shocks would capture sudden changes in the number of new infection cases, which people perceive as the rise in infection risk, which is reflected in changes in the degree of fear and anxiety about the COVID-19. The identified structural shocks would have historically captured changes in people's perception of infection risk, over the sample period.

Fig. 7 displays the time series of permanent and non-permanent shocks. The bars in the upper and lower panels indicate permanent and non-permanent shocks, respectively, as identified using the estimated VAR model. The orange shaded areas show the weeks coinciding with the period during the declaration of a state of emergency in

[23] Blanchard and Quah (1989) and King et al. (1991) develop the VAR model to identify structural shocks, by imposing restrictions on the long-run effect of a given shock on a given variable.

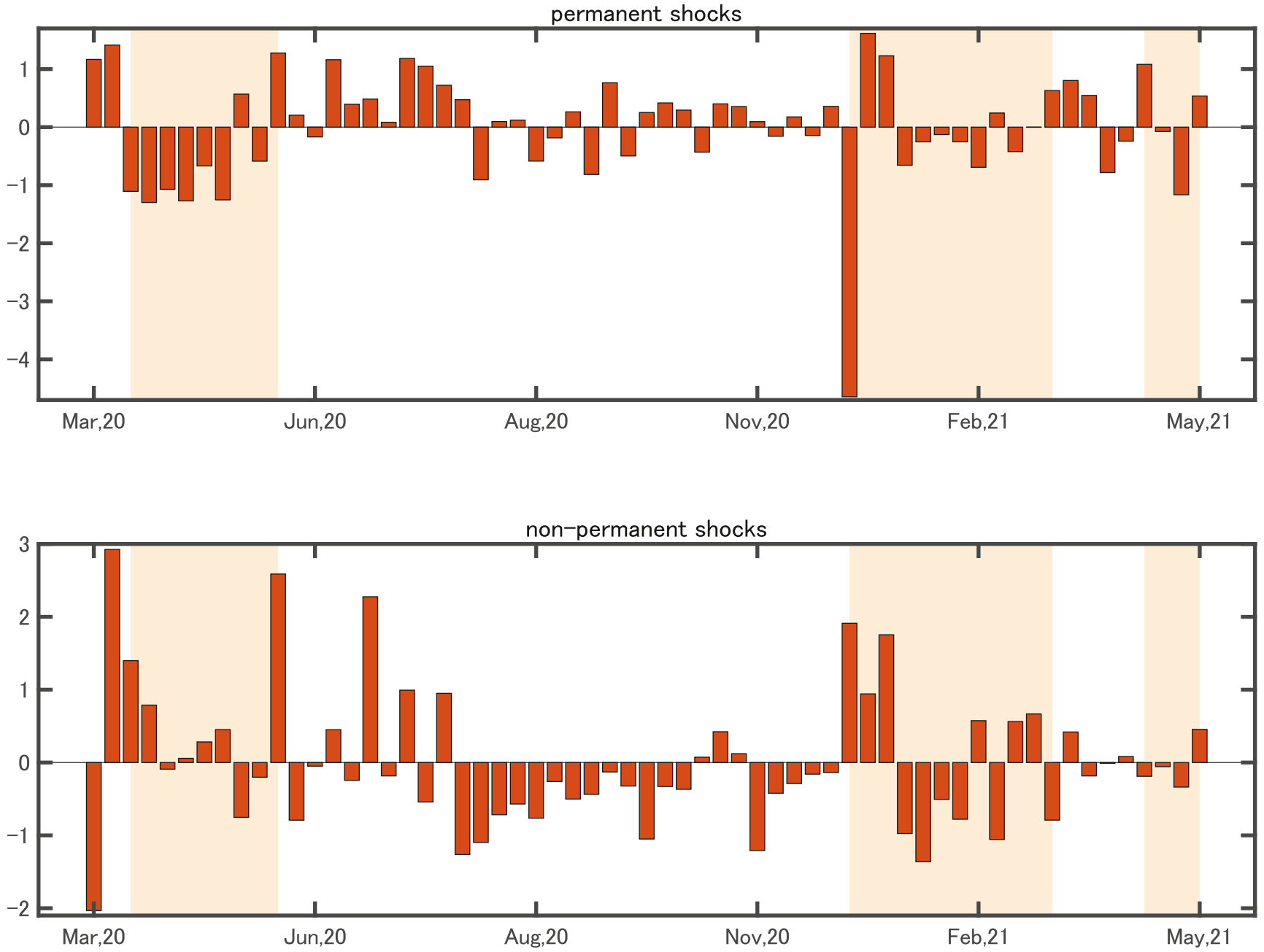

Fig. 7. Identified permanent and non-permanent shocks. *Notes*: The bars in the upper and lower panels indicate the permanent and non-permanent shocks, respectively, identified using the estimated vector autoregressive (VAR) model (11) with the restriction (14). We set the lag length to three weeks in the reduced-form VAR estimation. The orange shaded areas show the weeks coinciding with the period during the state of emergency declaration in Japan. The sample period spans from the week of March 1, 2020, to the week of May 9, 2021.

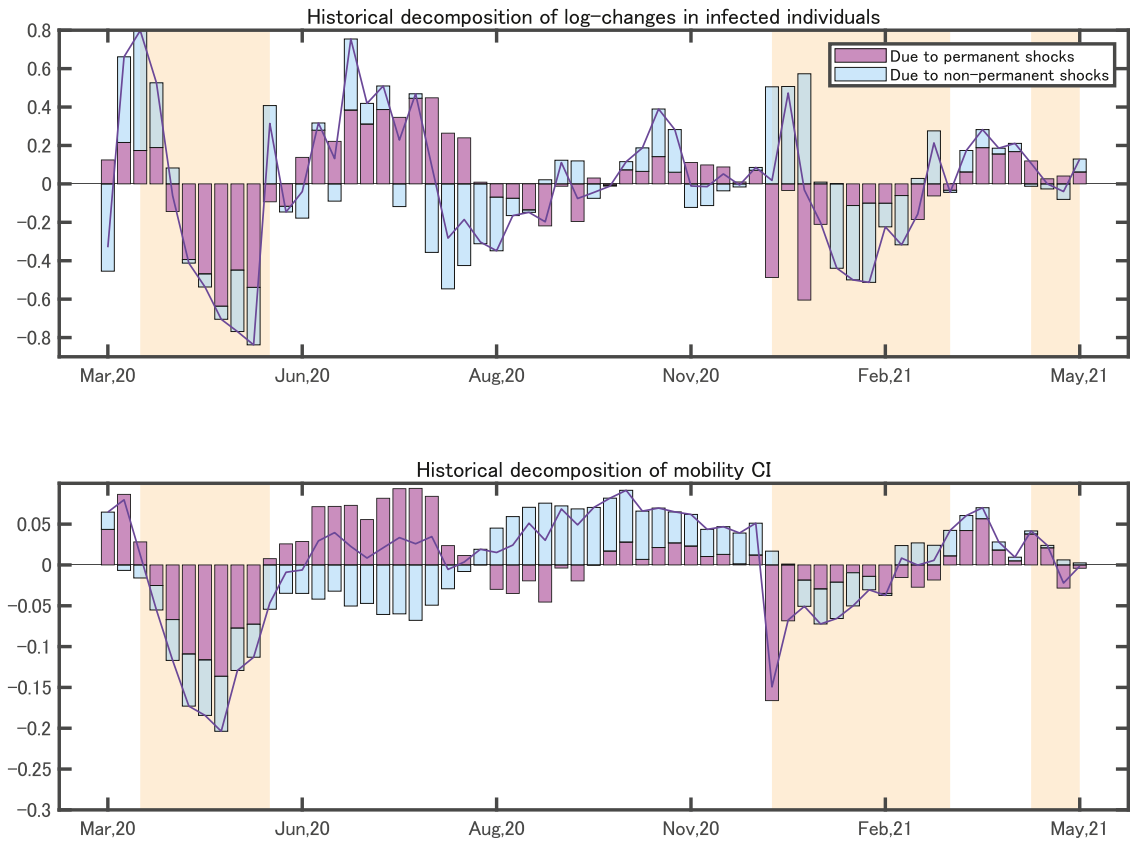

Fig. 8. Historical decomposition of changes in COVID-19 infection cases and human mobility due to permanent and non-permanent shocks. *Notes*: All the series are displayed as deviations from the deterministic component. Mobility CI denotes the composite index of mobility. The purple bar shows the decomposed series explained by the permanent shocks. The light blue bar shows the decomposed series explained by the non-permanent shocks. The solid line indicates the estimated stochastic component before decomposition. The orange shaded areas show the weeks coinciding with the period during the state of emergency declaration in Japan. We set the lag length to three weeks in the reduced-form vector autoregressive estimation. Estimation samples span from the week of March 1, 2020, to the week of May 9, 2021.

Japan.[24]

The upper panel of Fig. 7 shows the persistent troughs representing permanent shocks for the period during the first state of emergency declaration on April 7, 2020, followed by upward swings. Thus, the first state of emergency declaration can contribute to inducing a downward trend in the number of new infection cases in response to the first wave of the COVID-19 pandemic. Moreover, there are upward swings in permanent shocks for several weeks from the week of May 24, 2020, to the second half of August 2020. Hence, the termination of the state of emergency on May 25 may contribute to an upward trend in the number of new infection cases. However, there are no large troughs for the period during the second and third states of emergency, except for a significant drop at the week of the end of 2020. Therefore, the second and third states of emergency have not contributed to a decline in the number of new infection cases. Regarding non-permanent shocks, as in the lower panel of Fig. 7, we see persistent troughs from the first half of August 2020 to the second half of October 2020, and from the end of November 2020 to the end of December 2020.

We investigate the extent to which past movements in the new positive cases of COVID-19 infection and human mobility resulted from permanent or non-permanent shocks. Specifically, we use the historical decomposition technique to decompose the historical value of the log changes in new positive infection cases and the mobility index into the accumulated effects of current and past permanent or non-permanent shocks. The upper panel of Fig. 8 shows the time series of the log changes in new positive infection cases explained by permanent and non-permanent shocks, whereas the lower panel of the figure shows the time series of the composite index of mobility explained by the shocks. The purple bar shows the decomposed series explained by the permanent shocks, $\xi_{p,t}$, and the light blue bar shows the decomposed series explained by non-permanent shocks, $\xi_{c,t}$. The solid line indicates the estimated stochastic components before decomposition.

The results reveal that sources of the epidemics of the COVID-19 infection vary greatly from time to time. From the upper panel of Fig. 8, much of the fluctuation in the log changes in infection cases, during and several weeks after the first state of emergency declaration, occur due to permanent shocks. However, much of this fluctuation also stems from non-permanent shocks beginning in the first half of August. Even during the second and third states of emergency, a decline in the

[24] In Japan, a state of emergency was declared three times during the sampling period: from April 7 to May 25, 2020; from January 8, to March 21, 2021; and from April 25, 2021 onward. The legal basis for policy responses by governors of prefectures subject to the emergency measures is the "Act on Special Measures for Pandemic Influenza and New Infectious Diseases Preparedness and Response." Under the first declaration of emergency, prefectural governors were able to request that people refrain from going out of their homes, and to request and instruct facility administrators of schools, social welfare facilities, and entertainment venues to restrict the use of those facilities in accordance with the provisions of Article 45 of the Act. However, the Act does not stipulate any penalties for disobeying the instructions under Article 45, and Japan's curfew was extremely loose compared to the lockdowns in China, the United States, and many European countries, for example. On February 13, 2021, during the second declaration of a state of emergency, the Act was amended to allow prefectural governors to order facility managers. Based on the newly established Article 79, facility managers who do not comply with the order will be subject to a fine of up to 300,000 yen.

Table 5
A fraction of the forecast error variance explained by permanent or non-permanent shocks for COVID-19 infection cases and human mobility

	Log changes in infection cases		Composite index of mobility	
Horizon	Permanent	Non-permanent	Permanent	Non-permanent
0	18.6	81.4	92.8	7.2
4	51.4	48.6	71.1	28.9
8	48.3	51.7	62.1	37.9
20	48.1	51.9	61.9	38.1

Notes: The entries show the percentage variance of the forecast error made in the column variable, as explained by the permanent or non-permanent shock at a given horizon. The results are computed from the vector autoregressive (VAR) model (11) with the restriction (14) over the sample period from the week of March 1, 2020, to the week of May 9, 2021. We set the lag length to three weeks in the reduced-form VAR estimation.

log changes in infection cases stems from non-permanent shocks.

Finally, we assess the relative contributions of permanent and cyclical components for COVID-19 infection cases and human mobility dynamics. Specifically, given the permanent and non-permanent shocks in the VAR model, we decompose the forecast error variances of the log changes in infection cases and the composite index of mobility into the variances of permanent and non-permanent shocks. Next, we estimate the percentage contribution of each shock to the forecast errors of the log changes in infection cases and the composite index of mobility.

Table 5 presents the results of the forecast error variance decomposition. The relative contribution of non-permanent shocks to the fluctuations of the log changes in infection cases at the current week is about 80%. Although this contribution falls to about 50% at a longer horizon, the results suggest an important role of the permanent and non-permanent shocks in the dynamics of COVID-19 infection cases.

5.3. Role of human mobility in the dynamics of COVID-19 infection

In this subsection, we explore the role of human mobility in the dynamics of COVID-19 infection cases. We predict that the systematic response of human mobility generates the hump-shaped response of the changes in the new infection cases and the cyclicality therein. Thus, to investigate the plausibility of our prediction, we conduct counterfactual simulations using the VAR model developed by Bernanke et al. (1997) and Sims and Zha (2006) to measure the role of the systematic response of mobility in response to structural shocks.

First, we measure the dynamic effect of exogenous changes in human mobility. Specifically, we assume that the mobility changes, $\xi_{y,t}, t = 1, \cdots, T$, produce a unit increase in the composite index of mobility, with no impact on the log changes in infection cases at the time a shock occurs, due to epidemiological rigidity. Accordingly, we can calculate the impulse response functions to an exogenous mobility change as $B(L)\Theta_y$, where $\Theta_y = (0, 1)'$.

Fig. 9 shows the estimated impulse response function to an exogenous mobility change, $\widehat{B}(L)\Theta_y$. We find that, in response to an increase in human mobility, the log changes in infection cases remain roughly zero for two weeks, due to epidemiological rigidity, and then rapidly increase for eight weeks. The maximum impact is about four. Thus, a percentage increase in the composite index of mobility, which reflects a percentage increase in the mobility index with retail & recreation, raises the rate of new infection cases by approximately 4%. Hence, exogenous changes in people's behavior induce an increase in the number of new infection cases, along with an empirical trade-off relationship, reported in the next subsection.

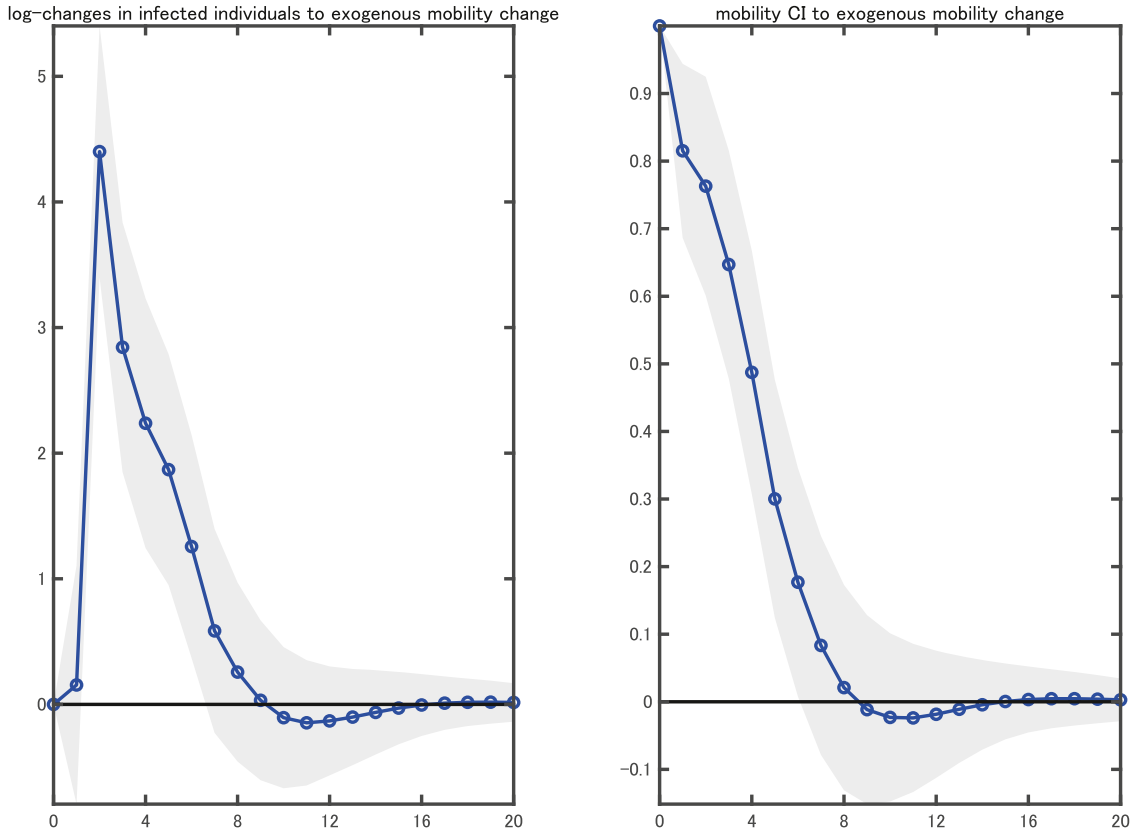

Fig. 9. Dynamic impacts of the exogenous mobility change on COVID-19 infection cases. *Notes*: The solid line with circles represents the point estimates of the impulse responses to an exogenous mobility change, $B(L)\Theta_y$, where $\Theta_y = (0, 1)'$. Mobility CI denotes the composite index of mobility. The mobility change increases the mobility CI by one unit. Estimation samples span from the week of March 1, 2020, to the week of May 9, 2021. The shaded areas denote one-standard-error bands, calculated using 1,000 bootstrap samples. We set the lag length to three weeks in the reduced-form vector autoregressive estimation.

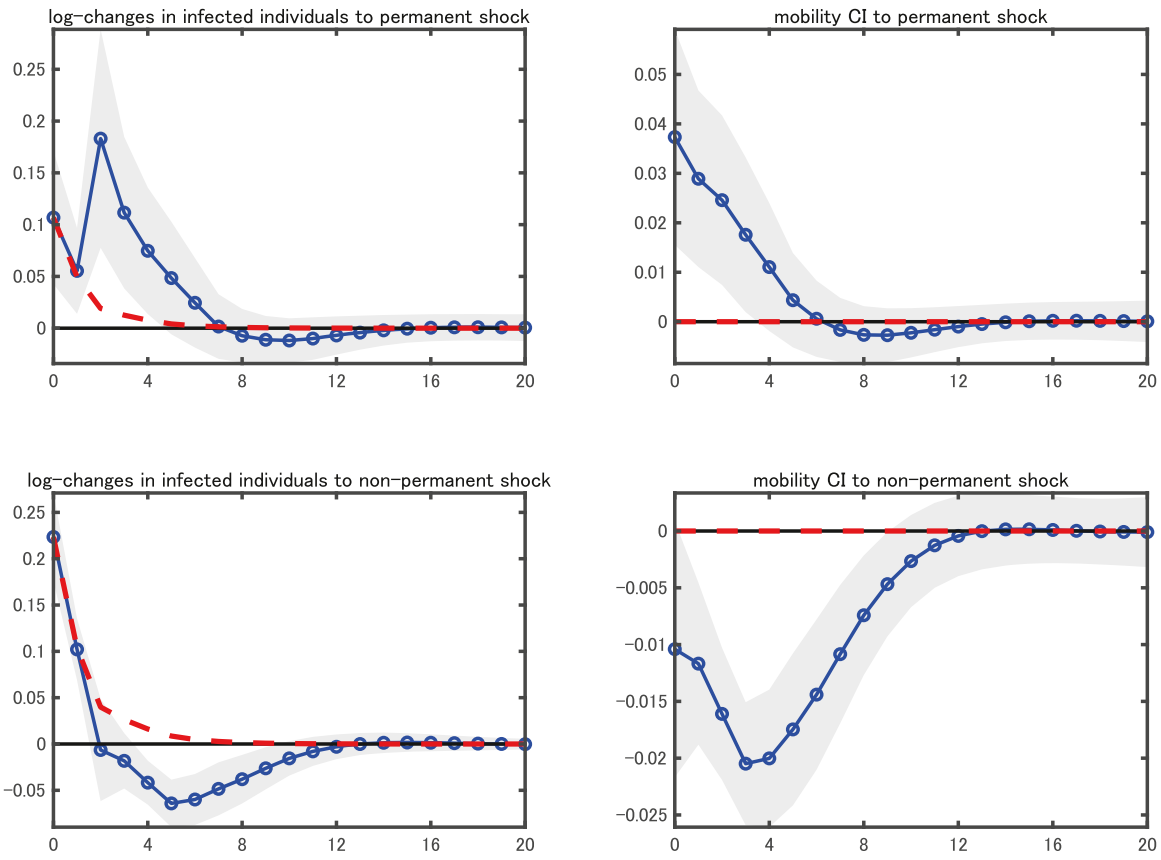

Fig. 10. Responses to permanent and non-permanent shocks, no mobility response. *Notes*: The solid line with circles in the upper and lower panels represent the point estimates of the impulse responses to one standard deviation permanent and non-permanent shock, respectively. The shaded areas denote one-standard-error bands, calculated using 1,000 bootstrap samples. The red dashed lines represent the simulated responses to each structural shock and sequence of mobility shocks to eliminate the normal response of mobility to the structural shocks. Mobility CI denotes the composite index of mobility. We set the lag length to three weeks in the reduced-form vector autoregressive estimation. Estimation samples span from the week of March 1, 2020, to the week of May 9, 2021.

Next, we investigate the role of human mobility in the dynamic response to COVID-19 infection cases given permanent and non-permanent shocks. Following Bernanke et al. (1997) and Sims and Zha (2006), we use the VAR model to conduct counterfactual simulations to assess how the number of new infection cases would have performed, without the systematic response of mobility to the structural shocks. Specifically, we measure the counterfactual values of the variables in the VAR model by taking the following steps. Given the response function to permanent and non-permanent shocks $B(L)\Theta_p, B(L)\Theta_c$, we calculate each sequence of exogenous mobility changes $\{\breve{\xi}^j_{y,0}, \breve{\xi}^j_{y,+1}, \cdots, \breve{\xi}^j_{y,+H}\}$ for $j = p$ and c that would reset $\breve{y}_0, \breve{y}_{+1}, \cdots, \breve{y}_{+H}$ to zero in response to permanent and non-permanent shocks, respectively. We then add each sequence before calculating the impulse response function of $\Delta\pi$ to permanent and non-permanent shocks.

Fig. 10 summarizes the simulation results. The red dashed lines represent the simulated responses to each structural shock and sequence of exogenous mobility changes, to eliminate the normal response of mobility to the structural shocks. The difference between the baseline result represented by the solid lines and the simulated result indicates a magnitude of the dynamic effect of the structural shocks through human mobility.

Our simulation results in the estimated VAR model are consistent with our model prediction in Section 3. From the upper-left panel of Fig. 10, the absence of mobility responses results in limited rise in the log changes in infection cases relative to the benchmark. Moreover, as in the lower-left panel of Fig. 10, the absence of mobility responses does not result in a continuous decline to converge to a steady-state level. These results of the macroeconometric analysis support the argument that human mobility creates an accelerated increase in new infection cases underlying the changes in its trend. Further, the systematic response of mobility demand automatically reduces the number of new infection cases underlying changes in its cycle.

5.4. Simultaneous equations system of infection-mobility trade-off and mobility demand

In this subsection, we examine the feasibility of our argument from another perspective. In Sections 5.2 and 5.3, we conducted a macroeconometric analysis on the premise of a stochastic trend and cycle in the new infection cases. We examined the dynamics of COVID-19 infection cases and human mobility to permanent and non-permanent shocks in the number of new infection cases, using the VAR model with a long-run restriction. While our dynamic model in Section 3 explains that the system comprising the infection–mobility trade-off and mobility demand can create the stochastic trend and cycle in the new infection cases, it is not obvious whether, in reality, the dynamics generated by permanent shocks and by non-permanent shocks employ the same system. Thus, we conduct another macroeconometric analysis using the VAR–IV model on the explicit premise of simultaneous equations comprising the infection–mobility trade-off and mobility demand.[25] We then show that we can explain the differences in the impact of permanent and non-permanent infection shocks in relation to the role

[25] See the online appendix for the derivation of the VAR–IV model from a simultaneous equationssystem of infection-mobility trade-off and mobility demand.

Table 6
Estimation results for the COVID-19 infection–mobility trade-off in Japan

Dependent variable:	log changes in infection cases
κ	3.28
	(0.54)
ι	0.09
	(0.05)
Adj-R^2	0.43

Notes: This table shows the ordinary least squares regression results (15) of the log changes in infection cases on the composite index of mobility and constant term. We obtain the composite index by scaling and signing the first principal component calculated using six Google mobility indices to the index for retail & recreation. The sample period spans from the week of February 23, 2020, to the week of May 2, 2021. The numbers in parentheses are Newey and West (1987) heteroskedasticity and autocorrelation robust standard errors for least squares with a four-week lag truncation.

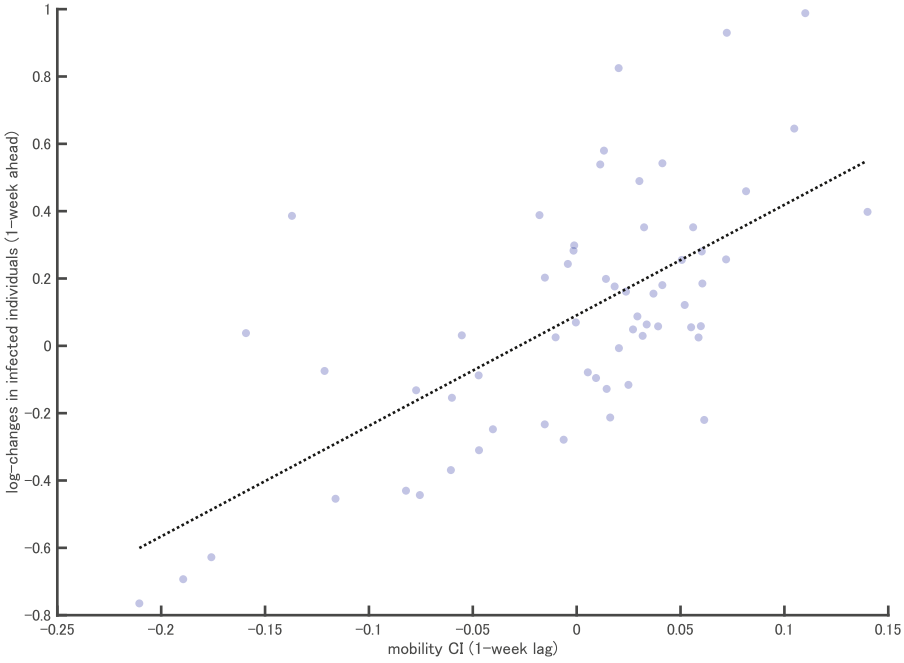

Fig. 11. Scatter plot of the log changes in infection cases and human mobility. *Notes*: Blue circles indicate the scatter plot of the one-week-ahead log changes in the number of COVID-19 infection cases and the one-week lag of the composite index of mobility. The dotted line indicates the fitted value for the regression of the one-week-ahead log changes in the number of infection cases on the one-week lag of the composite index of mobility based on the ordinary least squares estimation. Mobility CI denotes the composite index of mobility. The sample period spans from the week of February 23, 2020, to the week of May 2, 2021.

of mobility demand, in that the dynamics suggested by the empirical results employ the same mechanism as those described in the previous subsections.[26]

First, we empirically investigate the existence of the infection–mobility trade-off. Specifically, we estimate the following specification of the infection–mobility trade-off (1):

$$\Delta\pi_{t+1} = \kappa y_{t-1} + \iota + \epsilon_{\pi,t+1}. \tag{15}$$

The sample period spans from the week of February 23, 2020, to the week of May 2, 2021. Under the premise that the human mobility should be predetermined in the supply side of the infection cases due to the epidemiological rigidity, we can estimate the regression (15) by OLS.

Empirical evidence supports the existence of the trade-off between COVID-19 infection and human mobility. Table 6 reports estimation results for the infection–mobility trade-off (15). The coefficient κ describing the response of the one-week-ahead log changes in infection cases to the one-week lag of human mobility is positive and statistically significant for human mobility. The OLS estimate of κ implies that a percentage increase in the composite index of mobility raises the rate of new infection cases by about 3% after two weeks. It is quantitatively comparable with the finding using other mobility data and statistical models by Nagata et al. (2021).[27] Fig. 11 shows the scatter plot of the one-week-ahead log changes in the number of COVID-19 infection cases and the one-week lag of the composite index of mobility, which graphically confirms the stability of the positive relationship of COVID-19 infection cases and human mobility during the sample period.

Next, we empirically investigate the existence of the mobility demand. Specifically, we estimate the following specification of the mobility demand (5):

$$y_t = b\Delta\pi_t + \gamma' W_t + \xi_{md,t}, \tag{16}$$

[26] Note that the VAR model with a long-run restriction and the VAR–IV model should be considered to be inherently different from each other, as they have different restrictions. Nevertheless, as shown in the following analysis, we find that the dynamics estimated by using the VAR-IV model, are almost the same as those estimated by using the VAR with a long-run restriction.

[27] Nagata et al. (2021) report an impact of mobility changes in nightlife places on new confirmed cases of about 1% to 4%, despite large regional differences in sensitivity intensity.

Table 7
Estimation results for mobility demand in Japan

Dependent variable:	Mobility CI
OLS estimate of b	0.027
	(0.013)
IV estimate of b	-0.062
	(0.055)
Wald F	21.488
Hausman	2.764
	[0.096]

Notes: The dependent variable is the composite index of mobility. The independent variable is the log changes in infection cases. The constant and one- to three-week lags of log changes in infection cases and the composite index of mobility are included as control variables in the linear regression model. The ordinary least squares (OLS) estimate of b indicates the estimate of b by the OLS regression. The instrumental variable (IV) estimate of b indicates the estimate of b by the IV regression. We use the weekly log changes in the search volume of "感染者数" (number of infected individuals *in English*) in Google as an external instrument in the IV regression. The numbers in parentheses are White (1980) heteroskedasticity-robust standard errors. Coefficients and standard errors for the control variables are not reported. Wald F indicates White (1980) heteroskedasticity-robust F-statistic under the null hypothesis that the coefficient on the instrument from the first-stage regression of the log changes in infection cases on the instrument and control variables is equal to zero. Hausman indicates the statistic on the Hausman (1978) test under the null hypothesis that the OLS and IV estimators are consistent, but the OLS estimate is efficient. The numbers in brackets are p-values for the Hausman test. The sample period spans from the week of March 1, 2020, to the week of May 9, 2021.

where W_t is a vector of control variables comprising the one- to three-week lags of y_t and $\Delta\pi_t$ and a constant.[28] $\xi_{md,t}$ with a mean of zero and a variance of σ^2_{md} represents the nonsystematic component of the reaction of mobility demand, which we refer to as a "mobility demand shock." In interpreting the mobility demand shocks, $\xi_{md,t}$ may reflect transitory changes in the preferences of human behavior and emergent changes in human mobility patterns due to some prevalence measures, irrespective of whether they are compulsory or not, by the government.

We estimate the regression (16) by an instrumental variable (IV) estimation, because the number of infection cases can be contemporaneously positively correlated with mobility demand shock. For example, changing preferences for mobility, such as getting used to the pandemic lifestyle and experiencing complacency toward the COVID-19 outbreak, can make people more active, despite the worsening infection situation. Thus, the OLS estimate of b suffers from an upward endogeneity bias. However, estimation using an IV, such as surprise increases in new infection cases given the emergence of variant strains (which satisfies the relevance of the changes in infection cases and the exogeneity of the mobility demand shocks), allows for a consistent estimate of b.

The instrument in the analysis is the weekly log changes in the search volume of the Japanese term "感染者数" (number of infected individuals *in English*).[29] We expect this measure to reflect the degree of anxiety regarding the surprise changes in the spread of the COVID-19 infection among Japanese people, which correlates with the log changes in infection cases, but less so with familiarity/ignorance toward such cases.

To verify the robustness of the proposed instrument, we compute the F-statistic under the null hypothesis that the coefficient on the instrument from the first-stage regression of the log changes in infection cases on the instrument and control variables is equal to zero. We also conduct the Hausman (1978) test for endogeneity.

Table 7 reports the estimation results for the mobility demand (16). The coefficient b describing the systematic response of human mobility to the log changes in infection cases is negative (positive) in the IV (OLS) estimation. This result is consistent with our prediction that the OLS estimate of b suffers from an upward endogeneity bias. Moreover, the IV estimate of b shows that a percentage increase in new infection cases reduces the composite index of mobility by about 0.062, which is quantitatively comparable with the finding obtained by using other mobility data and the statistical model by Watanabe and Yabu (2021).[30] The instrument is robust, with a heteroskedasticity-robust first-stage F-statistic of 21.488.[31] Furthermore, the Hausman test result detects endogeneity of the log changes in infection cases, although at a 10% statistical level, possibly because of efficiency loss from the IV estimation. This result statistically supports the implication of our dynamic model, where the infection–mobility trade-off and mobility demand endogenously and simultaneously determine the number of new infection cases.

Next, we examine the dynamic effect of changes in anxiety related to surprise changes in the spread of COVID-19 infection. Let $\xi_{a,t}$ be an anxiety shock and Θ_a, the impact vector for the responses of the VAR variables X_t to the anxiety shock. We can express the impulse response functions of X_t to an anxiety shock $\xi_{a,t}$ as $B(L)\Theta_a$.

To identify $\Theta_a = (\Theta_{1a}, \Theta_{2a})'$, we adopt the VAR–IV model proposed by Stock and Watson (2012, 2018). Assume that a unit increase in $\epsilon_{a,t}$ increases $\Delta\pi_t$ by one unit $\Theta_{1a} = 1$. We use the IV regression to yield a consistent estimate of Θ_{2a}

$$e_{2,t} = \Theta_{2a} e_{1,t} + \xi_{md,t}, \tag{17}$$

using the instrument, where $e_{1,t}$ and $e_{2,t}$ are the reduced-form VAR innovations of the log changes in infection cases and the composite index of mobility, respectively. Given that the regression in Eq. (17) is

[28] In specifying the dynamics of human mobility, one might argue that log level should also be added to the VAR model. In particular, Chernozhukov et al. (2021) and Hoshi et al. (2021) find evidence that not only the log changes, but also the log levels of cases are an important determinant of mobility, using panel data for the US and Japan. Nevertheless, even with the addition of log level of cases, there should be a less significant difference in the mobility dynamics that can be captured by our VAR model. In the online appendix, we provide empirical results showing that adding log level of cases in our VAR model plays a limited role in explaining the dynamics of the composite index of mobility. It is important to note that we do not claim that our results are inconsistent with the findings of Chernozhukov et al. (2021) and Hoshi et al. (2021). We interpret that the detailed information contained in the log level of weekly cases in explaining the dynamics of human mobility is already contained in the lagged values of log changes of cases and human mobility in our VAR model. In addition, the results of our IV estimation of mobility demand, taking into account the presence of endogenous bias, are consistent with the claims of Chernozhukov et al. (2021) and Hoshi et al. (2021) that the higher number of cases reduced people's mobility.

[29] We retrieved the search volume data from Google Trends (https://trends.google.co.jp/trends/?geo=JP) on June 1, 2021.

[30] Given the result of the factor model in the online appendix, a percentage increase in new infection cases increases mobility in residence by $0.026(\simeq -0.062 \times -0.42)$. Watanabe and Yabu (2021) report a reduction in people's outings by 0.026% due to a 1% increase in new infection cases.

[31] To ensure that a weak instrument problem is not present, Stock et al. (2002) and Stock and Yogo (2005) recommend the rule of thumb that requires the F-statistic from the first-stage regression of the two-stage least squares to exceed 10.

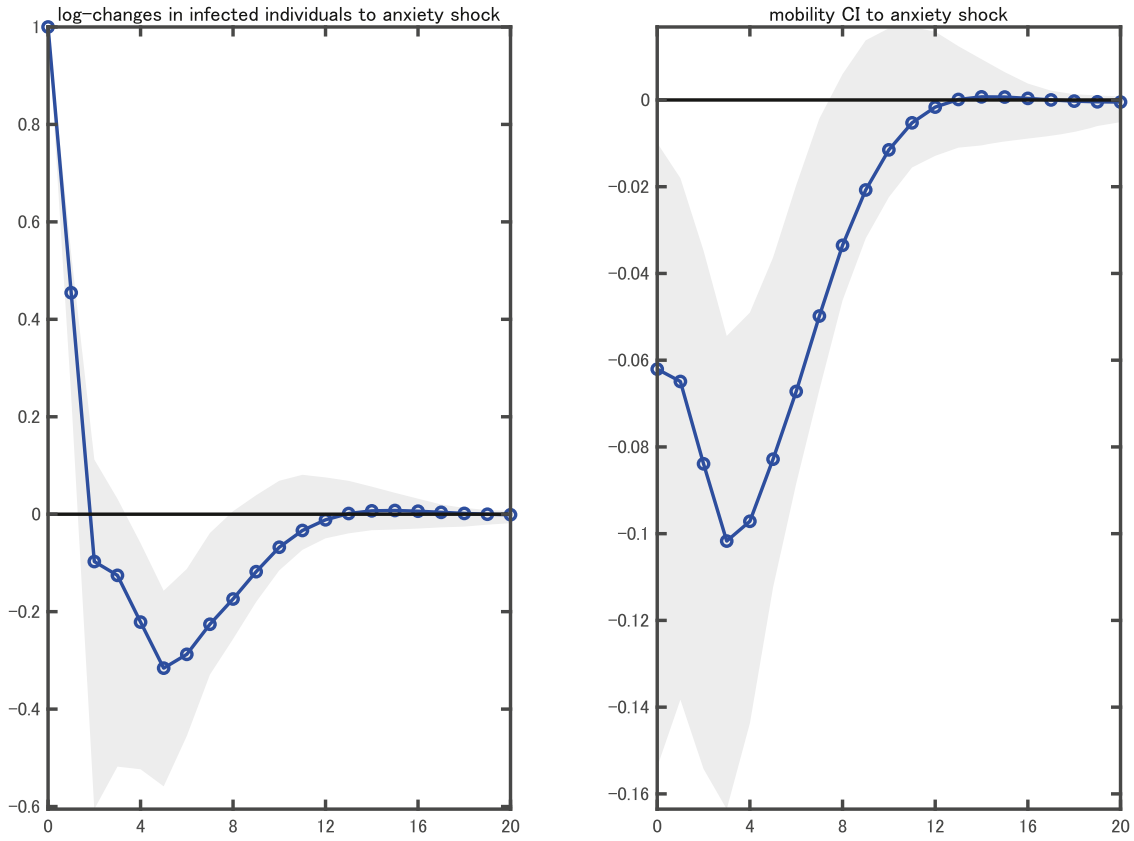

Fig. 12. Dynamic impacts of an anxiety shock on COVID-19 infection cases and human mobility. *Notes*: The solid lines with circles represent the point estimates of the impulse responses to an anxiety shock identified using the estimated vector autoregressive (VAR) model (11) with the weekly log changes in the search volume of "感染者数" (number of infected individuals *in English*) in Google as an external instrument. The anxiety shock increases the log changes in infection cases by one unit. The shaded areas denote one-standard-error bands, calculated using 1,000 bootstrap samples. Mobility CI denotes the composite index of mobility. We set the lag length to three weeks in the reduced-form VAR estimation. Estimation samples span from the week of March 1, 2020, to the week of May 9, 2021.

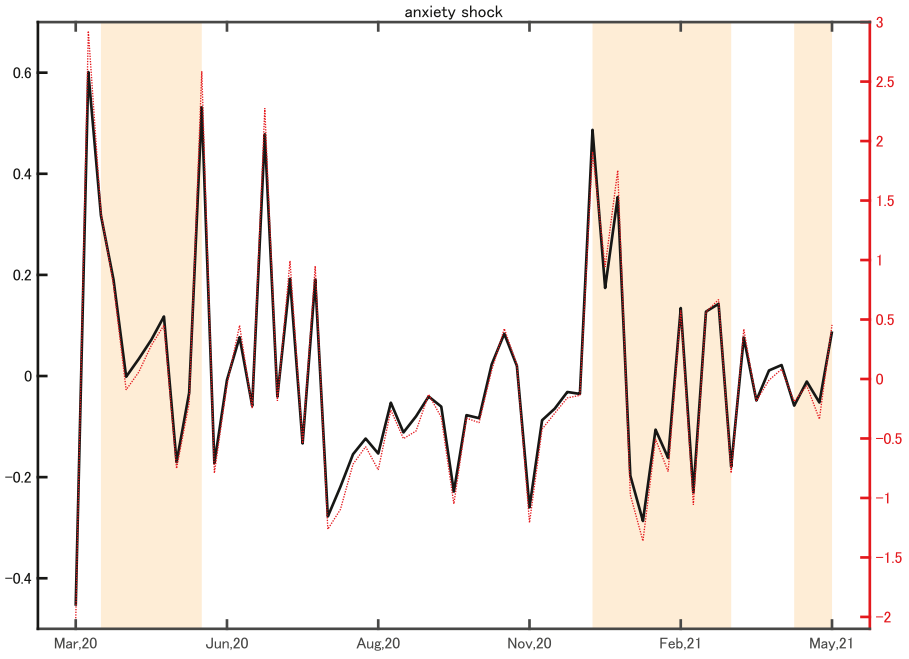

Fig. 13. Identified anxiety shocks. *Notes*: The solid line (left-hand scale) indicates the anxiety shocks identified using the estimated vector autoregressive (VAR) model (11) with the weekly log changes in the search volume of "感染者数" (number of infected individuals *in English*) in Google as an external instrument. The dotted line (right-hand scale) indicates the non-permanent shocks identified using the estimated VAR model (11) with the restriction (14). We set the lag length to three weeks in the reduced-form VAR estimation. The sample period spans from the week of March 1, 2020, to the week of May 9, 2021. The orange shaded areas show the weeks coinciding with the period during the state of emergency declaration in Japan.

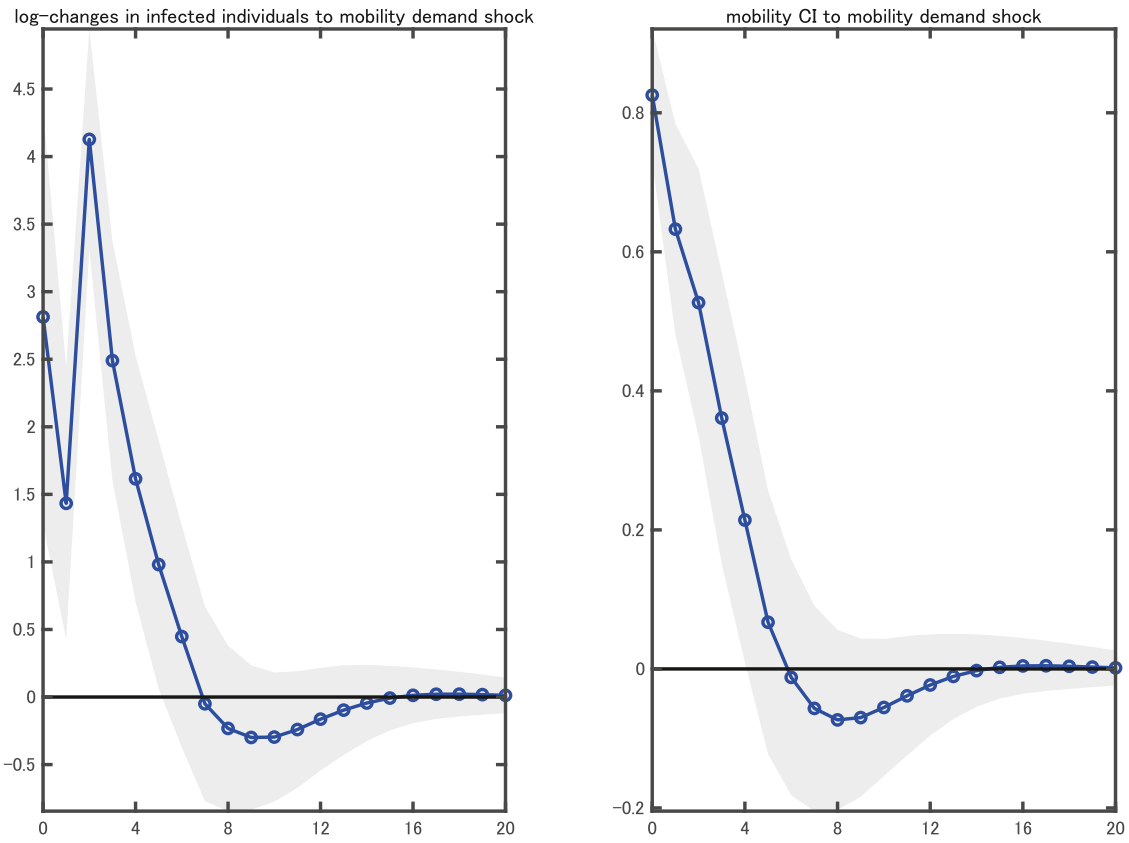

Fig. 14. Dynamic impacts of a mobility demand shock on COVID-19 infection cases and human mobility. *Notes*: The solid line with circles represents the point estimates of the impulse responses to one unit of a mobility demand shock obtained from the residual of the instrumental variable regression (16) with the weekly log changes in the search volume of "感染者数" (number of infected individuals *in English*) in Google as an instrument. The shaded areas denote one-standard-error bands, calculated using 1,000 bootstrap samples. Mobility CI denotes the composite index of mobility. We set the lag length to three weeks in the reduced-form vector autoregressive estimation. Estimation samples spans from the week of March 1, 2020, to the week of May 9, 2021.

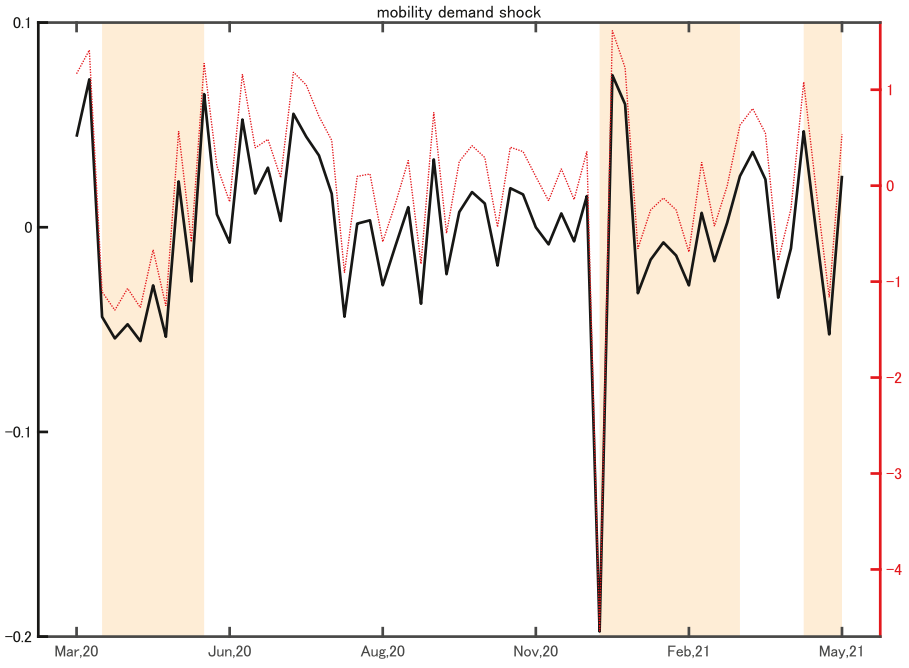

Fig. 15. Identified mobility demand shocks. *Notes*: The solid line (left-hand scale) indicates the mobility demand shocks obtained from the residual of the instrumental variable regression (16) with the weekly log changes in the search volume of "感染者数" (number of infected individuals *in English*) in Google as an instrument. The dotted line (right-hand scale) indicates the permanent shocks identified using the estimated vector autoregressive (VAR) model (11) with the restriction (14). We set the lag length to three weeks in the reduced-form VAR estimation. The orange shaded areas show the weeks coinciding with the period during the state of emergency declaration in Japan. The sample period spans from the week of March 1, 2020, to the week of May 9, 2021.

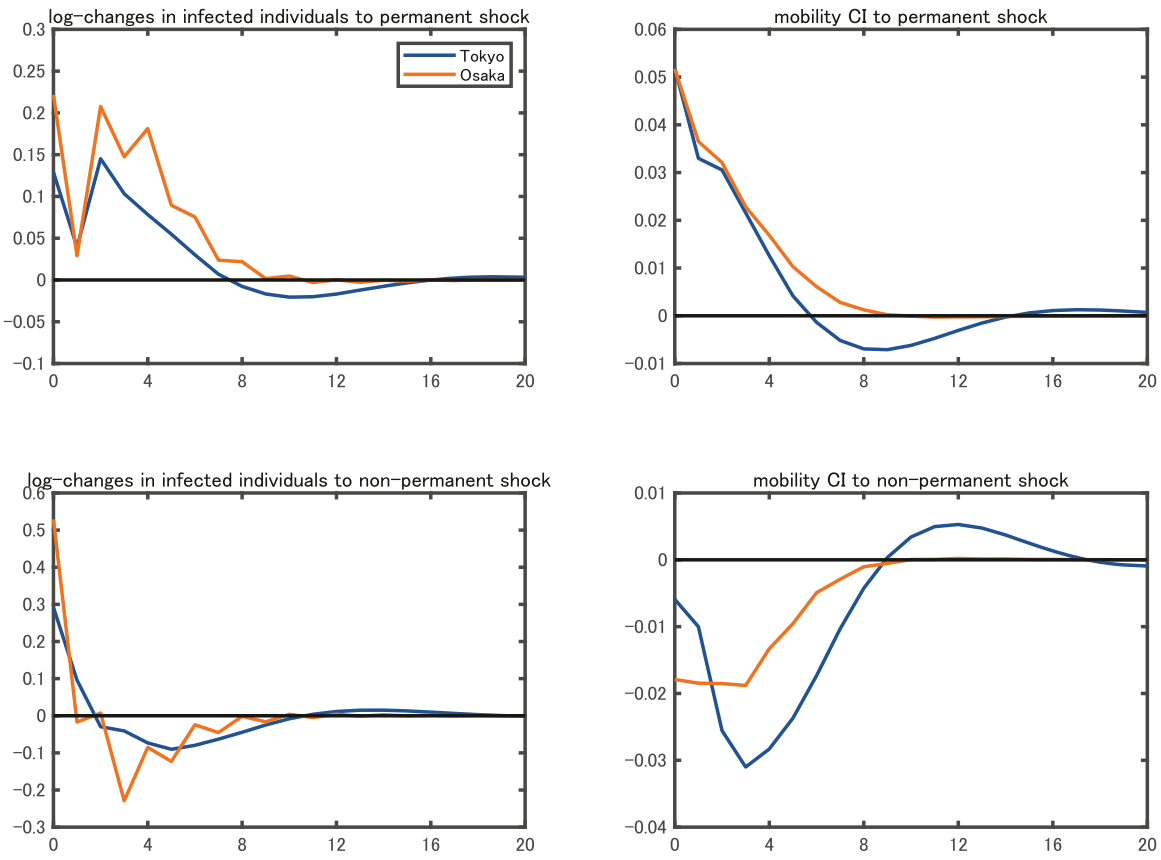

Fig. 16. Estimated responses of the log changes in infection cases and human mobility to permanent and non-permanent shocks in Tokyo and Osaka. *Notes*: The solid lines in the upper and lower panels represent the point estimates of the impulse responses to one standard deviation permanent and non-permanent shock, respectively, by prefecture. Mobility CI denotes the composite index of mobility. We set the lag length to three weeks in the reduced-form vector autoregressive estimation. Estimation samples span from the week of March 1, 2020, to the week of May 9, 2021. Different colors represent different prefectures, where the navy blue is for Tokyo and the dark orange is for Osaka.

mathematically equivalent to the regression in Eq. (16), we can set Θ_{2a} as the IV estimate of b.

Fig. 12 summarizes the estimated impulse response functions $\widehat{B}(L)\widehat{\Theta}_a$. Accordingly, a unit increase in infection cases due to an anxiety shock leads to a persistent decrease in human mobility to its lowest values approximately four weeks after the shock occurs. Moreover, after the transitory rise in the log changes in infection cases for two weeks, they decline steadily for about eight weeks. These responses are qualitatively similar to those regarding a non-permanent shock reported in Fig. 6.

We can confirm that the anxiety shocks identified by the VAR–IV model are the same as the non-permanent shocks identified by the VAR model with long-run restriction. Fig. 13 displays the time series of anxiety shocks indicated by the solid line (left-hand scale). Relative to the time series of non-permanent shocks (the dotted line, right-hand scale) identified with the long-run restriction (14), the two series are observationally equivalent (the Pearson's correlation coefficient between them is 0.997), except for the size of variances. This evidence implies that the space covered by the anxiety shocks should cover the space of the non-permanent shocks identified by imposing the long-run restriction. Therefore, it supports our view that a systematic response of mobility demand to a surprise change in the new infection cases generates the cyclicality of COVID-19 infection cases.

Finally, we examine the dynamic impact of a mobility demand shock on COVID-19 infection cases and human mobility. The straightforward way to analyze it within our framework is to include the shocks obtained from the IV regression (16) in the VAR as an exogenous variable:

$$A(L)X_t = a_0 + \Theta_{md}\xi_{md,t} + e_t^{\perp}, \tag{18}$$

where Θ_{md} is a two-by-one vector capturing the contemporaneous response of the elements of X_t to a mobility demand shock. The innovation term $e_t^{\perp}$ is, by construction, orthogonal to the mobility shock. We can obtain the consistent estimates of Θ_{md} by regressing the VAR innovations e_t on the mobility demand shocks $\xi_{md,t}$. We can express impulse response functions of X_t to a mobility demand shock $\xi_{mb,t}$ as $B(L)\Theta_{md}$.

In addition to the anxiety and non-permanent shocks, the mobility demand shocks are the same as the permanent shocks identified in the VAR model with the long-run restriction. From Fig. 14, the estimated responses to a mobility demand shock are qualitatively similar to those to a permanent shock. In response to the rise in human mobility due to a mobility demand shock, the log changes in infection cases have a hump-shaped response, with the second peak effect occurring after two weeks. Moreover, from Fig. 15, the mobility demand shocks track the movement of the permanent shocks precisely, which changes the stochastic trend in the new infection cases. Thus, the changes in mobility demand, such as the changes in human behavioral preferences and emergent changes in human mobility patterns, can accelerate changes in the stochastic trend in new infection cases.

The results can reconcile highly controversial evidence on the

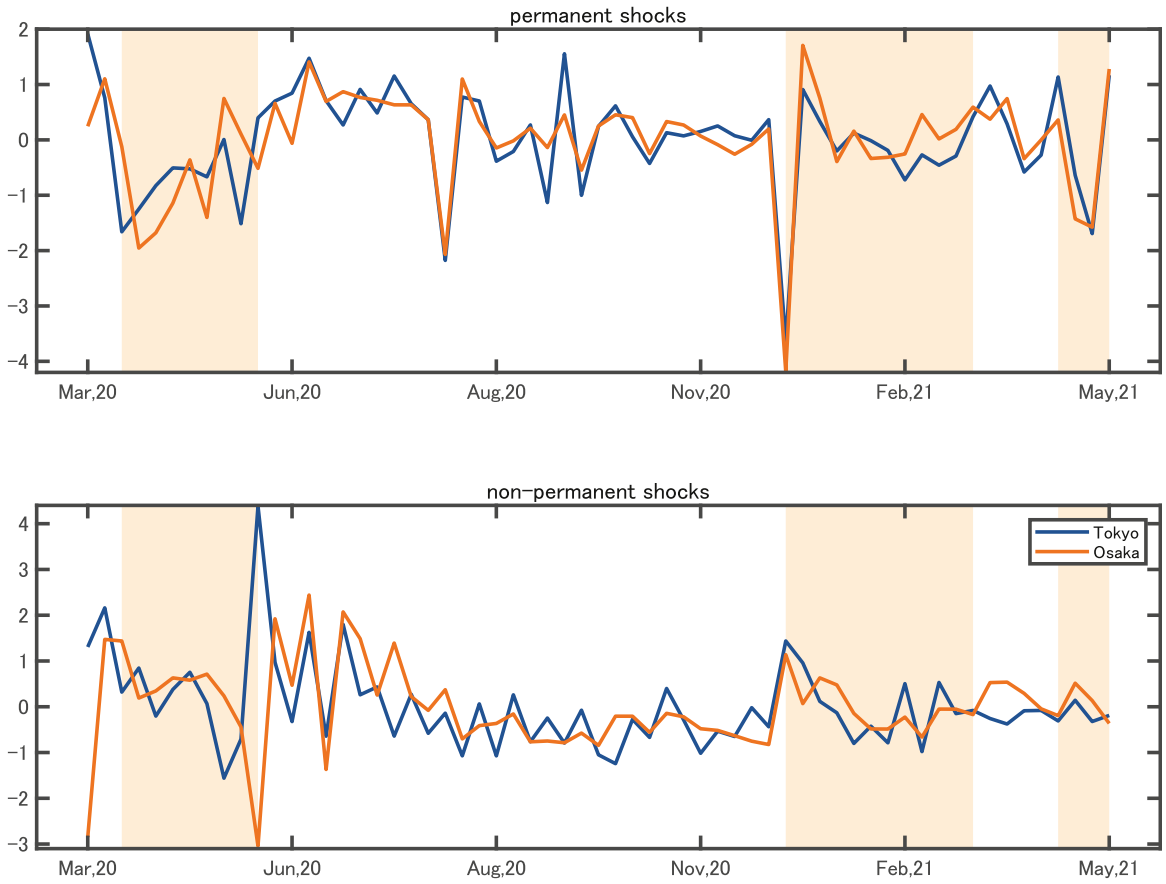

Fig. 17. Identified permanent and non-permanent shocks in Tokyo and Osaka. *Notes*: The solid lines in the upper and lower panels indicate the permanent and non-permanent shocks, respectively, identified using the estimated vector autoregressive (VAR) model (11) with the restriction (14) by prefecture. We set the lag length to three weeks in the reduced-form VAR estimation. The orange shaded areas show the weeks coinciding with the period during the state of emergency declaration in Japan. The sample period spans from the week of March 1, 2020, to the week of May 9, 2021. Different colors represent different prefectures, where the navy blue is for Tokyo and the dark orange is for Osaka.

association between COVID-19 infection cases and human mobility. Studies such as Kraemer et al. (2020) and Nagata et al. (2021) report empirical evidence on the positive causal relationship between human mobility and infection cases. Others, such as Goolsbee and Syverson (2021) and Watanabe and Yabu (2021), report empirical evidence on the negative causal relationship between human mobility and infection cases. Our proposed simultaneous equations system, which takes into account the two causal relationships between human mobility and new infections, can interpret these conflicting empirical results without contradiction, and is useful for understanding infection dynamics. Therefore, analyses using macroeconometrics provide a more realistic picture of the COVID-19 infection cases and human mobility to capture the role of the stochastic trend and cycle in their dynamics.

5.5. Application to the infection situation in Japanese prefectures

In this subsection, we present the empirical results of applying our empirical framework to time-series data of new infection cases in Japanese prefectures.[32] In particular, we investigate whether there is a dynamic causal relationship as obtained in section 5.2 for these regional time-series data. We further illustrate how regional differences in the evolution of an infection situation can be interpreted in our framework.

We limit our analysis to the infection situation in the two prefectures of Tokyo and Osaka, where the number of the new infection cases is relatively high, compared to elsewhere in Japan.[33] Both of these prefectures experienced a sustained decrease in the infection cases during the state of emergency declaration, and a persistent increase in cases after the state of emergency declaration was lifted. Nevertheless, there are regional differences in the infection spread. In particular, when the first emergency declaration was lifted, the infection situation in Osaka improved steadily, and the emergency declaration was lifted earlier on May 21, but the infection situation in Tokyo was not reassuring.[34] Also, after the second state of emergency declaration was lifted, the infection

[32] We thank an anonymous referee for suggesting the following analysis.

[33] In the online appendix, we take a look at the evolution of an infection situation in Tokyo and Osaka to illustrate a common trend and regional differences in infection spread.

[34] On June 2, 2020, immediately after the first state of emergency declaration was lifted, the Tokyo Metropolitan Government issued "Tokyo Alert," its own standard for providing warning signals regarding the infection spread situation of COVID-19, for the first time, to warn Tokyo residents about signs of a resurgence of the infection.

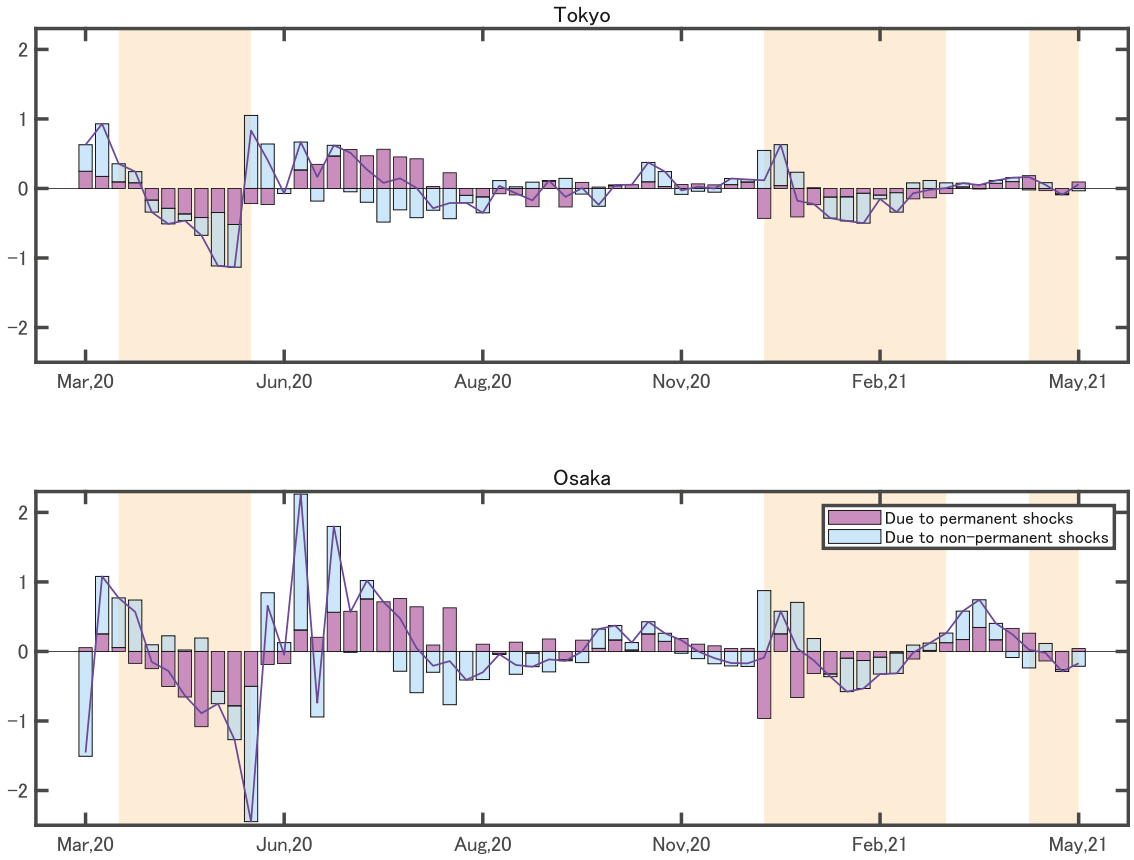

Fig. 18. Historical decomposition of log changes in COVID-19 infection cases due to the permanent and non-permanent shocks in Tokyo and Osaka. *Notes*: All the series are displayed as deviations from the deterministic component. The purple bar shows the decomposed series explained by the permanent shocks. The light blue bar shows the decomposed series explained by the non-permanent shocks. The solid line indicates the estimated stochastic component before decomposition. The orange shaded areas show the weeks coinciding with the period during the state of emergency declaration in Japan. We set the lag length to three weeks in the reduced-form vector autoregressive estimation in each prefecture. Estimation samples span from the week of March 1, 2020, to the week of May 9, 2021.

situation in Osaka deteriorated rapidly.[35]

We apply our empirical framework to the infection situation in each prefecture. Specifically, we estimate the VAR model with a long-run restriction separately, using the time-series data of the log changes in infection cases and human mobility in each prefecture. As well as carrying out an analysis with the aggregated data, we construct the composite index of mobility for each prefecture, using six of Google's mobility indices and employ it as an endogenous variable in the VAR model.[36] The one- to three-week lags of the endogenous variables are included in the VAR model for each prefecture.

Fig. 16 shows the estimated impulse response of the log changes in infection cases and the composite index of mobility to permanent and non-permanent shocks in Tokyo and Osaka. We find that, although there are quantitative regional differences, the estimated dynamic causal relationship between the infection cases and human mobility is qualitatively similar to the results for Japan as a whole in section 5.2; a permanent infection shock causes a hump-shaped increase in infection cases with increased human mobility and a non-permanent shock causes a temporary increase in cases with decreased human mobility.

Fig. 17 displays the time series of identified permanent and non-permanent shocks in Tokyo and Osaka. As seen in the top panel of the figure, we find that the permanent shocks tend to occur simultaneously across the two prefectures.[37] On the other hand, as seen in the bottom panel of the figure, we find that the time series of non-permanent shocks vary considerably between Tokyo and Osaka.[38] In particular, there is a large discrepancy between the non-permanent shocks in Tokyo and Osaka at the end of the first and second states of emergency declarations. This implies that the source of the differences in the evolution of an infection situation between the two prefectures, can be interpreted as occurring primarily due to non-permanent shocks in our framework.

Fig. 18 gives the historical decomposition of the log changes in infection cases in Tokyo and Osaka. We find that the decomposed series explained by permanent shocks is similar to the ones in the upper panel of Fig. 8. In particular, there is a common tendency in the two prefectures for the decomposed series to drop significantly during the first state of emergency declaration, and to rise significantly in the weeks following the lifting of the declaration. Nevertheless, we find that the fluctuation in the decomposed series explained by non-permanent shocks is considerably larger than that explained by permanent shocks. This implies that when analyzing the relationship between infection spread and human mobility using prefecture-specific data, variations in the growth rate of new cases by prefecture is likely to be

[35] In Osaka, the second state of emergency declaration was lifted ahead of schedule, on February 28, 2021. However, in response to the reemergence of the infection, on April 7, the Osaka Prefectural Government called for the prefectural residents to be vigilant, stating that the infection situation was at the most serious level based on the "Osaka Model," its own standard for a warning signal regarding the infection spread situation of COVID-19.

[36] See the online appendix for the time-series data on the composite index of mobility in Tokyo and Osaka that we use in the analysis.

[37] We confirm that there is a statistically positive correlation of permanent shocks between Tokyo and Osaka (correlation coefficient is 0.81).

[38] The correlation of the non-permanent shocks between Tokyo and Osaka is small, with a correlation coefficient of 0.11.

dominated by the influence of non-permanent shocks.

The application in this subsection suggests the importance of monitoring the changes in people's perception of infection risk, in controlling infection spread throughout Japan. The infection spread can vary from prefecture to prefecture, but much of it is temporary, thanks to people in each prefecture curbing their mobility. On the other hand, permanent shocks, possibly due to exogenous changes in mobility demand, may create a common tendency of infection spread across prefectures. Policymakers may need to intervene to limit people's behavior if the infection spread is expected to be long-lasting and widespread, as people's perception of the infection risk changes.

6. Summary and discussion

Human mobility is pivotal in considering the dynamics of the number of COVID-19 infection cases. Arguably, there is a trade-off between the increase in new infection cases and human mobility. The number of new infection cases increases, because the probability of susceptible people being infected by interacting with other infected people becomes higher as more people move around. However, there is a systematic response of mobility demand regarding the new infection cases; that is, when the number of new infection cases increases, people restrain their mobility. Hence, there is a stochastic trend and cycle in the infection dynamics. As described in our analysis using the dynamic model of COVID-19 infection and human mobility, human mobility can create an acceleration of the spread of COVID-19 infection and its cyclicality under the simultaneous relationship.

This study has provided empirical evidence in support of the argument. Using time-series data from February 2020 to May 2021 in Japan, we demonstrated the stochastic trend and cycle in the new infection cases. Using macroeconometric analysis applied to the time series of log changes in the new infection cases and human mobility, we demonstrated the feasibility of our predictions. Moreover, sources of the COVID-19 infection spread vary significantly from time to time, and the changes in the trend and cycle of the new infection cases explain approximately half of its variation, respectively, from March 2020 to May 2021 in Japan.

The findings of this study offer suggestions on some of the current concerns regarding COVID-19. For instance, there is concern that the infection rate may vary from time to time, because the severe acute respiratory syndrome coronavirus 2, an RNA virus, is prone to mutation. The emergence of a variant strain would cause surprise changes in the new infection cases, reflecting a transitory change in the parameter κ in our model. Nevertheless, we predict that if we respond appropriately to the situation and change our behavior, we can keep the number of new infection cases at a certain level, under the premise of system stability.

However, the primary concern of this study is that, as the COVID-19 infection spread continues, people may ignore the situation, and partly or fully continue (or resume) economic activities because they have become accustomed to living amid the reality of the pandemic and a life of restrictions. Through this study, we hope to curb the speed of infection spread by helping people realize that how they regulate their behavioral preferences and freedom of mobility can reduce the probability of infections. Such decisions are reflected in practical measures such as wearing masks, avoiding close encounters, social distancing, and refraining from going out if one has COVID-19-related symptoms, to stall the spread as much as possible. Admittedly, despite the fact that the declaration of a state of emergency due to the spread of the COVID-19 infection and the request to refrain from needlessly going out have greatly restricted economic activities, Japan has not experienced a major medical collapse, and the probability of people in the country contracting the virus has been kept extremely low. However, people are likely to be wearied by the repeated declarations of a state of emergency and calls for self-restraint. If this scenario becomes unbearable and people begin ignoring the situation, the number of infection cases could increase exponentially.

Hence, what actions can be taken to prevent an escalation of the infection rate? Assuming that economic activities continue, it would be challenging to completely control the spread of infections, and a certain level of new infection cases will be inevitable. People must act to avoid increasing the number of new infection cases, due to the changes in their preferences regarding systematic behavior. Even without relying on strict countermeasures against COVID-19 infections, avoiding a sustained increase in the number of new infection cases via people's behavioral responses, is possible by employing the practical measures highlighted above.

Although this study assumes a stable system, structural changes are expected.[39] In particular, we expect the widespread administration of vaccines to cause a structural change in the parameter κ, in that it becomes flat in our model, thereby inducing a weak trade-off between the new infection cases and human mobility. Nevertheless, if the widespread availability of vaccines changes people's preferences in terms of ignoring the situation, which pushes the parameter in the mobility demand, b, toward zero in our dynamic model, then the spread of COVID-19 infections may emulate the seasonal flu epidemics in winter. As of June 2021, when this paper was being prepared, this speculation is consistent with events in countries where vaccines are widely available.

There are many possibilities for an extension of the analysis in this study, leaving room for future research to proceed in several directions. First, investigating the system stability in the dynamics of the number of new infection cases is an important theoretical and empirical challenge. Although our analysis is premised on cyclicality and the stochastic trends in new infection cases, the model predictions and empirical results do not necessarily hold for every economy. The dynamics in our model strongly depend on the set of its parameters. In particular, as the parameter representing the systematic response of mobility demand to the new infection cases, b, tends toward zero, the model predicts less cyclicality in such cases. Thus, the irresponsibility of human mobility in the economy is associated with the probability of an infection explosion, which can vary significantly by country and region, depending on behavioral factors such as testing and quarantine procedures for positive cases, lifestyle, and culture. Hence, future research can theoretically examine conditions that are satisfied with cyclicality in the new infection cases and quantitatively assess its degree, using time-series data in other countries and regions.

Second, although this study considers the formation of the reference level of new infection cases briefly in the models, future studies can provide empirical evidence on the formation of people's opinions and beliefs regarding the reality of epidemics. The study's findings present important policy implications. An important task for policymakers in predicting and controlling infections is to monitor changes in people's perception of infection risk. If people continue to ignore the risk of infection and engage in economic activities, policymakers should take interventions that will change the way people view the risk of infections. To do so, we need to consult quantitative assessments on *how* people form their opinions and beliefs regarding the reality of epidemics. It is also important to extend the model to include the policy sector, in order to analyze the role of policy interventions, such as a systematic control

[39] It would be interesting to analyze the fourth wave and the subsequent decline of COVID-19 in Japan. At this time, vaccination in Japan progressed rapidly. We speculate that the widespread use of vaccines may have played a major role in the decrease in the number of cases after the fourth wave. However, because there is little data after the vaccine has been distributed throughout Japan, it is difficult to verify the structural changes in the VAR model. Therefore, we leave the analysis of possible structural changes in the system as a future issue.

of human mobility in response to increases or decreases in the number of new infections.[40] Moreover, significant heterogeneity in the level of concern people have about the situation is expected. It is conceivable that those who are at high risk of serious illness may respond to government measures and requests to refrain from economic activities, while those at low risk may ignore them.

Finally, the study findings can encourage important developments in building epidemiological models incorporating human behavior. From the theoretical analysis in Gans (2020), in environments where the systematic responses of mobility demand to changes in the number of new infection cases fully work, an equilibrium level would be reached long before herd immunity is achieved. However, even in the SIR–Macro model, as in Eichenbaum et al. (2021), where the reproduction rate systematically changes depending on economic activities, this mechanism seems to be unattractive. Better predictions and simulations of new infection cases may be provided by modifying the SIR models, implying an economically convenient reduction in the reproduction rate.

Appendix A. Data sources and weekly data construction

Data on the new confirmed cases of COVID-19 and the Oxford Stringency Index are obtained from Our World in Data.[41] The Oxford Stringency Index is calculated by the Oxford Coronavirus Government Response Tracker project.[42] This index averages nine indices: school closures, workplace closures, cancellation of public events, restrictions on public gatherings, closures of public transport, stay-at-home requirements, public information campaigns, restrictions on internal movements, and international travel controls. Each index takes a value from 0 to 100. The larger the index, the stricter the government's response.

Data on the new confirmed cases in Tokyo and Osaka are obtained from the Japan Broadcasting Corporation (NHK) special website for new coronaviruses[43] because the data on COVID-19 Data Repository by CSSE at Johns Hopkins University, which is the source for Our World in Data, have missing values for the sample period from February 16, 2020, to May 9, 2021. We confirm that both data are consistent except for the missing values.

The mobility indices are from the COVID-19 Community Mobility Reports by Google.[44] Each mobility variable is calculated as the rate of deviation from the reference value, which is set for each day of the week. The reference value for each day of the week, is the median value for each day of the week for five weeks, from January 3 to February 6, 2020.

The frequency of all data is daily. We convert to weekly data from Sunday to Saturday, in order to eliminate the transitory factor. The number of new weekly infection cases and the weekly mobility indices, are calculated as the cumulative number of new daily infection cases and the median of the daily mobility indices each week, respectively.

Supplementary material

Supplementary material associated with this article can be found, in the online version, at 10.1016/j.jjie.2022.101195

References

Arik, S.O., Li, C.-L., Yoon, J., Sinha, R., Epshteyn, A., Le, L.T., Menon, V., Singh, S., Zhang, L., Yoder, N., Nikoltchev, M., Sonthalia, Y., Nakhost, H., Kanal, E., Pfister, T., 2020. Interpretable Sequence Learning for COVID-19 Forecasting. 34th Conference on Neural Information Processing Systems, NeurIPS 2020.
Atkeson, A., 2020. What will be the economic impact of COVID-19 in the US? Rough Estimates of Disease Scenarios. NBER Working Paper.March. No.26867
Atkeson, A., Kopecky, K., Zha, T., 2020. Four stylized facts about covid-19. NBER Working Paper.August. No.27719
Bernanke, B.S., Gertler, M., Watson, M.W., 1997. Systematic monetary policy and the effects of oil price shocks. Brook. Paper. Econ. Activ. 28 (1), 91–142.
Blanchard, O.J., Quah, D., 1989. The dynamic effects of aggregate demand and supply disturbances. Am. Econ. Rev. 79 (4), 655–673.
Chernozhukov, V., Kasahara, H., Schrimpf, P., 2021. Causal impact of masks, policies, behavior on early COVID-19 pandemic in the U.S. J. Econo. 220 (1), 23–62.
Cochrane, J.H., 1988. How big is the random walk in GNP? J. Polit. Econ. 96 (5), 893–920.
Eichenbaum, M.S., Rebelo, S., Trabandt, M., 2021. The macroeconomics of epidemics. Rev. Financ. Stud. 34 (11), 5149–5187.
Fujii, D., Nakata, T., 2021. COVID-19 and output in japan. Japan. Econ. Rev. 72, 609–650.
Fukao, M., Shioji, E., 2022. Is there a tradeoff between covid-19 control and economic activities? implications from the phillips curve debate. Asian Econ. Policy Rev. 17 (1), 66–85.
Gans, J.S., 2020. The economic consequences of $\tilde{R} = 1$: Towards a workable behavioural epidemiological model of pandemics. Covid Econ.: Vett. Real-Time Papers 41, 28–51.
Goolsbee, A., Syverson, C., 2021. Fear, lockdown, and diversion: Comparing drivers of pandemic economic decline 2020. J. Publ. Econ. 193, 104311.
Hamilton, J.D., 1994. Time Series Analysis. Princeton: Princeton University Press.
Hausman, J.A., 1978. Specification tests in econometrics. Econometrica 46 (6), 1251–1271.
Hoshi, K., Kasahara, H., Makioka, R., Suzuki, M., Tanaka, S., 2021. Trade-off between job losses and the spread of COVID-19 in japan. Japan. Econ. Rev. 72 (4), 683–716.
Hosono, K., 2021. Epidemic and economic consequences of voluntary and request-based lockdowns in japan. J. Japan. Int. Econ. 61, 101147.
Jiang, F., Zhao, Z., Shao, X.,. forthcoming. time series analysis of COVID-19 infection curve: A change-point perspective. J. Econ..
King, R.G., Plosser, C.I., Stock, J.H., Watson, M.W., 1991. Stochastic trends and economic fluctuations. Am. Econ. Rev. 81 (4), 819–840.
Kissler, S., Tedijanto, C., Lipsitch, M., Grad, Y.H., 2020. Social distancing strategies for curbing the COVID-19 epidemic. medRxiv.
Kraemer, M.U.G., Yang, C.-H., Gutierrez, B., Wu, C.-H., Klein, B., Pigott, D.M., du Plessis, L., Faria, N.R., Li, R., Hanage, W.P., Brownstein, J.S., Layan, M., Vespignani, A., Tian, H., Dye, C., Pybus, O.G., Scarpino, S.V., 2020. The effect of human mobility and control measures on the COVID-19 epidemic in china. Science 368 (6490), 493–497.
Kubota, S., 2021. The macroeconomics of COVID-19 exit strategy: The case of japan. Japan. Econ. Rev. 72, 651–682.
Kuga, N., 2021. 'corona habituation' and weakening of infection fears – infection fears weakened after peaking in winter, while infection re-emerged (in japanese). Kisoken Lett.(

(久我尚子「「コロナ慣れ」と感染不安の弱まり – 感染再拡大の一方、冬をピークに弱まる感染不安」基礎研レター　2021-04-23　ニッセイ基礎研究所)

)
Lauer, S.A., Grantz, K.H., Bi, Q., Jones, F.K., Zheng, Q., 2020. The incubation period of coronavirus disease 2019 (COVID-19) from publicly reported confirmed cases: Estimation and application. Am. College Phys.
Nagata, S., Nakaya, T., Adachi, Y., Inamori, T., Nakamura, K., Arima, D., Nishiura, H., 2021. Mobility change and COVID-19 in japan: Mobile data analysis of locations of infection. J. Epidemiol. 31 (6), 387–391.
Newey, W.K., West, K.D., 1987. A simple, positive semi-definite, heteroskedasticity and autocorrelation consistent covariance matrix. Econometrica 55 (3), 703–708.
Sims, C.A., 1980. Macroeconomics and reality. Econometrica 48 (1), 1–48.
Sims, C.A., Zha, T., 2006. Does monetary policy generate recessions? Macroecon. Dyn. 10 (2), 231–272.
Stock, J.H., Watson, M.W., 2012. Disentangling the channels of the 2007-2009 recession. Brook. Paper. Econ. Activ. 44 (1), 81–135.
Stock, J.H., Watson, M.W., 2018. Identification and estimation of dynamic causal effects in macroeconomics using external instruments. Econ. J. 128 (610), 917–948.
Stock, J.H., Wright, J.H., Yogo, M., 2002. A survey of weak instruments and weak identification in generalized method of moments. J. Bus. Econ. Stat. 20 (4), 518–529.
Stock, J.H., Yogo, M., 2005. Testing for weak instruments in linear IV regression. pages 80–108 of: In: Andrews, D.W.K., Stock, J.H. (Eds.), Identification and Inference in Econometric Models: Essays in Honor of Thomas J. Rothenberg. Cambridge University Press, Cambridge.
Watanabe, T., Yabu, T., 2021. Japan's voluntary lockdown. PLos ONE 16 (6).e0252468
White, H., 1980. A heteroskedasticity-consistent covariance matrix estimator and a direct test for heteroskedasticity. Econometrica 48 (4), 817–838.

[40] Fukao and Shioji (2022) use the system comprising the infection–economic activity trade-off, people's choice of economic activity levels, as well as a policy reaction, and point out the importance of a trade-off between economic activities and COVID-19 infection cases in understanding the role of public policies.
[41] https://ourworldindata.org/
[42] https://covidtracker.bsg.ox.ac.uk/
[43] https://www3.nhk.or.jp/news/special/coronavirus/
[44] https://www.google.com/covid19/mobility/